HEAT MANAGEMENT ALTERNATIVES IN DEEP UNDERGROUND MINES AS A CRUCIAL PART OF MINE VENTILATION

by

Mohit Butani

A Thesis Submitted to the Faculty of the

DEPARTMENT OF MINING AND GEOLOGICAL ENGINEERING

In Partial Fulfillment of the Requirements

For the Degree of

MASTER OF SCIENCE

In the Graduate College

THE UNIVERSITY OF ARIZONA

2021

THE UNIVERSITY OF ARIZONA
GRADUATE COLLEGE

As members of the Master's Committee, we certify that we have read the thesis prepared by: MOHIT BUTANI
titled: HEAT MANAGEMENT ALTERNATIVES IN DEEP UNDERGROUND MINES AS A CRUCIAL PART OF MINE VENTILATION

and recommend that it be accepted as fulfilling the thesis requirement for the Master's Degree.

Moe Momayez
Moe Momayez Date: Aug 10, 2021

Krishna Muralidharan Date: Aug 11, 2021

Muhammad Waqas
Muhammad Waqas Date: Aug 10, 2021

Final approval and acceptance of this thesis is contingent upon the candidate's submission of the final copies of the thesis to the Graduate College.

I hereby certify that I have read this thesis prepared under my direction and recommend that it be accepted as fulfilling the Master's requirement.

Moe Momayez
Moe Momayez Date: Aug 10, 2021
Thesis Committee Chair
Department of Mining and Geological Engineering

ACKNOWLEDGEMENTS

I want to express my immense appreciation to my academic supervisor and mentor, Dr. Moe Momayez, for his immense contribution, guidance, and support throughout this research. Dr. Moe has provided me with inspiring guidance, constructive criticism, and valuable suggestions throughout these 2 years. I am very much thankful to him for his guidance and pain-taking effort in improving my understanding of this project. I learned a lot by working with him on this project.

I also want to thank my co-supervisor, Dr. Muralidharan Krishna, for guiding me through Molecular Dynamics simulations and the result interpretations. I also want to thank Dr. Muhamad Waqas for taking his time to be a part of the committee member and giving his reviews for the thesis. My honest and sincere thanks to Dr. Pratish Rao for his time and efforts to guide me through the experimental side of the project. Without his experimental analysis, it would have been challenging to complete this research. I also want to thank the National Institute for Occupational Safety and Health (NIOSH) for providing financial support to conduct this research. Special thanks to David Streeter for providing technical support at the lab. A big thanks to Sherri Raskin for providing information regarding the courses, classes, jobs/internship, and completing all paperwork for the degree completion.

Finally, I would like to thank my family members and all my friends for their constant support throughout my journey here and for being beside me through thick and thin.

DEDICATION

I would like to dedicate this to my parents, Dr. Gurmukh Butani and Mrs. Meera Butani, and my complete family for supporting me throughout my journey. Today I am here because of your guidance and support.

Table of Contents

TABLE OF FIGURES

LIST OF TABLES

ABSTRACT

The thermal transport properties of porous amorphous aluminosilicate structures are investigated using molecular dynamics simulations and finite element methods. This research aims to produce such aluminosilicate geofoam of desired thermal conductivity and use it as sprayable thermal insulation in deep mines or potentially in residential insulation applications. Aluminosilicates are naturally occurring minerals which have low thermal conductivity because of their high porosity. Since they are found in abundance in nature, they could be an economical alternative for the fabrication of thermal insulators used in the buildings and underground mines. The thermal and mechanical properties of the amorphous porous aluminosilicate structures (PAS) were studied during this research using computational and experimental methods. Molecular dynamics (MD) was used to characterize thermal properties and conductivity at the atomic level. Different Aluminum-Silicon ratios were studied in molecular dynamics to identify a suitable Al-Si ratio that would provide lowest possible thermal conductivity and high mechanical strength. The effect of density on thermal conductivity was also characterized. It was observed that thermal conductivity of the alumino silicate structure has a linear dependency on density. Also, for a particular given porosity, a larger distribution of smaller pores results in the aluminosilicate structure to have a lower thermal conductivity. This characteristic is related to the presence of more phonon scattering centers in highly porous systems thus causing a decrease in the mean free path of a phonon. The data obtained from the molecular dynamics simulations was used to physically fabricate the foams with similar densities in the laboratory and their associated thermal conductivity was experimentally measured. The molecular dynamics simulations and experimental data show a high degree of agreement with each other.

The ultrasound non-destructive technique (NDT) was used to transmit wave energy to measure dynamic mechanical properties experimentally. This was performed for various different porosities of foams. The foam density was changed using different ratios of blowing agent and surfactant. The same was performed using the finite element method analysis in COMSOL Multiphysics platform for different sets of porosities. Acoustic and stress analysis was performed for different porosities to determine the P-wave and S-wave velocities and other elastic properties. A high-fidelity model of the foam was also generated using a micro-CT scan of the foam. Volume meshing was performed using Simpleware ScanIp software and was then transferred over to COMSOL to perform the modelling simulations. The data from different porosities obtained from these simulations agrees very well with the findings in the experimental analysis.

The research involves the characterization for morphology via SEM and chemical bonding by NMR synthesis of low-density foams with density as low as 0.22 g/cc. Also, the thermal conductivity values that have been obtained are seen to be a function of density of the material by transient plane source method. The mechanical properties have been characterized by Ultrasonic tests for macroscopic bulk specimens and techniques such as AFM at the Nanoscale and the results are hereby reported.

CHAPTER 1: INTRODUCTION

1.1 Background

Heat insulation has been in use since ages. From the hot sun outside in the desert heat of Southwest United States to the cold weathers in Northeast United States. Insulation is key to maintaining a temperature and keep the heat where it is supposed to be. The quality of insulation has a direct effect in the amount of energy used to generate heating/cooling in the places of habitat. In other words, if your house loses heat to the cold outside, you need more energy to continue to spend more energy to keep the inside of the house hot. Similarly, if it is hot outside and the walls of your house do not insulate very well, then the heat from the outside will get inside the house through walls and heat up the inside of the house. Heat will always travel from a place of higher temperature to a place of lower temperature. To combat this, one will have to spend more energy to cool down or heat up the house constantly. Here is where an insulator comes in handy. An insulator will keep the heat where it is supposed to be and reduce the amount of energy spent into heating or cooling of the house. The best part of an insulator is that it works passively and doesn't require any energy to function itself.

In a solid, during conduction, as the atoms vibrate more from the added heat, those vibrations are transferred to the atoms next to it and they pass it to atoms next to them and so on. This phenomenon of heat transport through a solid is referred as a vibration characteristic of that material and is called a Phonon. The longer it takes a phonon to travel through a material from the edge at a higher temperature to an edge with a lower temperature, the lower its thermal conductivity. Air itself is a very good insulator if heat and hence is the go-to approach to reducing thermal conductivity is introducing a lot of air within a certain material. Take for

example the polar bear, the fur of animals which live in the extreme cold climates are the reason why they survive in that cold weather. Their fur traps huge amount of air between their body and the cold air outside. This blanket of air provides them with the thermal insulation required to survive and maintain a body temperature required to live normally. The same concept is applied to the insulations between the walls of a well-insulated house, there are materials like fiberglass, cellulose, mineral wool, polystyrene, phenolic foam etc. that are basically ways to trap a bunch of air within to use as insulation **Error! Reference source not found.**. The exact same p henomenon is used in the sweater that people wear. It comes out logical to use air as an insulator since it is light in weight and is omnipresent. We followed the same ideology in this research.

The demand for minerals continues to grow. As there is a limit to safely and economically operate an open-pit mine as we progress deeper from surface, the only way forward to continue mining is to go for underground mining. One of the biggest challenges that is faced in deep underground mines are the sources of heat. There are numerous heat sources in deep underground mines like auto compression of air, heat from machinery, heat from explosives while blasting, etc., but the most prominent one being the geothermal heat, as seen in Fig. 1.

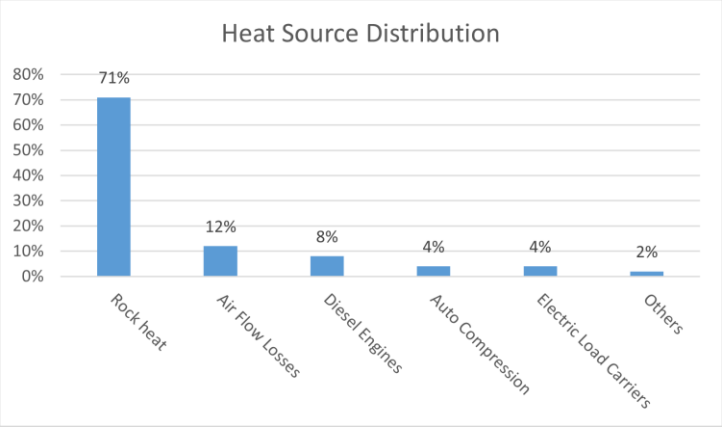

Fig. 1 - Typical heat sources in Underground Mines (adapted from Vergne, 2008) [4].

Geothermal gradient is the increase in the strata temperature with depth. It is given as a rate of increase in temperature with change in depth. This gradient leads to heat flow from the hot rocks to the colder areas, which in this case are the mine airways. The thermal gradient is about 25°C/km of depth for the first 3-5 kilometers of depth under the earth's crust [2]. Now, these high temperatures in the deep underground mines make it impossible for humans to work there comfortably. Which is why, a lot of energy is spent into cooling the mines to make it comfortable for humans to work in, as seen in fig 2.

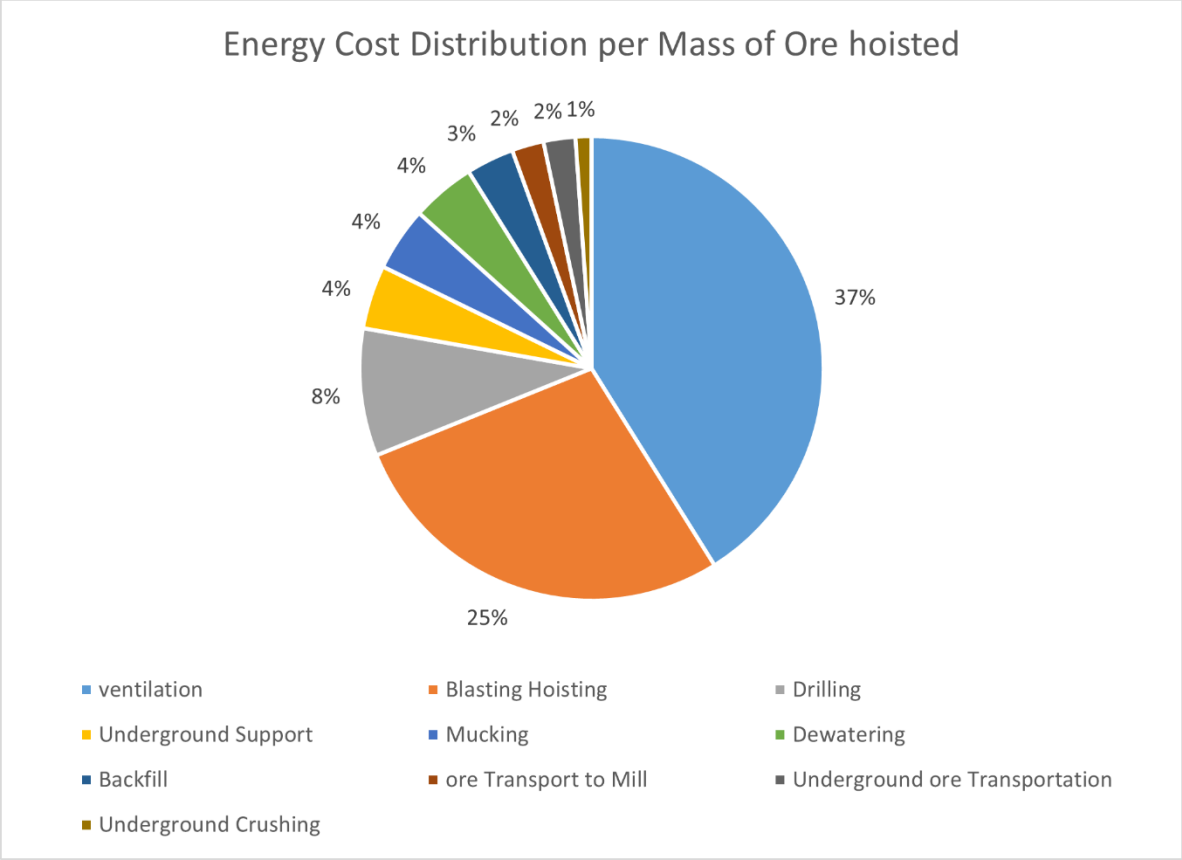

Fig. 2 - Cost Energy Comparison between Total Mine Operation and Mine Ventilation (adapted from CIPEC, 2005) [4]

In hot underground mines, the heat flow from the strata into the mine workings is proportional to the difference between the rock temperature and the air temperature. Mine ventilation is thus very important to maintain a hazard-free work environment for maximum efficiency and

productivity. We can also equip mine workers with unconventional cooling systems like cooling vests [3] or cooling watches, but the effects are only temporary. This is a huge setback as the cost of operations keep increasing the deeper we go and this will again restrict mining from economics point of view. Since cost is one of the biggest driving forces in the mining industry, and this not being a small operation as just one house, the cost of doing it the way it is done in houses will not be very cost effective, hence, it is important to look for cheap alternative solutions to keep the costs down and still get the job done safely. This research is oriented towards exploring options to use waste materials from the mines to produce these insulating substances. Porous aluminosilicate material was identified with having the potential to achieve this goal.

This study is a part of a larger research project that explores an alternate and relatively cost-effective solution to slow down the transfer of geothermal heat using a robust aluminosilicate precursor in a ceramic foam. The foam is highly porous and will serve as an insulator between the heat in the rocks and the mine airways. It will be sprayed on the mine walls in the form of shotcrete.

1.2 Challenges of the mining industry

Geothermal heat is just one of the challenges of the deep underground mining industry. Other challenges include Physical disturbances to landscape, Public Safety, Air Contamination, Soil and Water Contamination [5].

Fig. 3 - Image of a Mine Tailings Dam [6]

Mine tailings are challenging in terms of their storage and disposal. If not regulated and efficiently managed, these could contribute to environmental pollution and have detrimental effects causing accidents leading to economic damage and even fatalities.

Mine tailings are byproducts consisting of mixed rocks and processing fluids formed after extracting valuable metals, minerals, etc. [7]. The byproducts after the treatment include many compounds like in the following table, and it is evident that oxides of Silicon, Aluminum and Iron are predominant in its concentration [8][9].

Compound	Copper Mine Tailings Weight%	Gold Mine tailings Weight%
SiO2	64.8	49.9
Al2O3	7.08	10.4
Fe2O3	4.33	9.7
CaO	7.52	11.1
MgO	4.06	5.9
SO3	1.66	-
Na2O	0.9	3
K2O	3.26	1.3
TiO2	-	1.3

Table 1 – The composition of Copper and Gold Mine Tailings [8][9]

1.3 Research Objectives

Given all the discussion above, the objective of this research is two-fold. One, to control the geothermal heat entering the mine airways from the mine walls. And two, to recycle the minerals found in mine tailings to fabricate the aluminosilicate structure to be used in mines. Being able to do this will save a lot of money in the mining operation costs, it will reduce the overall environmental impact of the mines and on top of that it will cool down the mines and improve the working efficiency of the workers in the mine due to the colder environment. Therefore, this is a triple win-win situation.

Initially, pristine materials, that is pure alumina and pure silica are used to develop control sets and to minimize the complexities arising from the presence of impurities in mine tailings.

Previous research on ceramic foams indicates a strong correlation between its thermal and mechanical properties with the amount of porosity introduced in the sample. Therefore, porosity is considered a study parameter to investigate the thermal conductivity and mechanical properties to optimize the foam's synthesis process.

This thesis focuses on studying the mechanical and thermal properties of the aluminosilicate structure with the following objectives:

1. Adapt the foam fabrication process developed by Dr. Pratish Rao to replicate on the new sonicator and adapt to be able to create larger batches.
2. Study thermal conductivity by Molecular Dynamics simulations on Alumino-Silicate structure with the Si:Al ratio of 4:1 and add to the previous data sets

3. Study the Velocity correlation function of vibration of all atoms in the Alumino-Silicate structure with Si:Al is equal to 3:1 to find out the phonon vibration characteristics of the material
4. Calculating Young's Modulus of porous aluminosilicate structure using molecular dynamics simulations
5. Calculating Young's Modulus of the Alumino-Silicate structure using COMSOL Multiphysics at higher frequency of P-waves and S-waves

Parts of this thesis are from the following papers that I have contributed in.

[A] Gaurav Gupta, Akash Chaurasia, Moe Momayez, Pratish Rao, Krishna Muralidharan, Mohit Butani, "Estimation of Thermal Conductivity of Porous Aluminosilicates Using Molecular Dynamics Simulations"

[B] Pratish Rao, Akash Chaurasia, Moe Momayez, Krishna Muralidharan, Mohit Butani, "Evaluation of Mechanical Properties of Alumino Silicate Foam by Ultrasound Transmission Technique"

CHAPTER 2: ALUMINOSILICATES

2.1 Why Aluminosilicates

Silicon and Aluminum are the among the most abundant elements found in the earth's crust and they often combine with oxygen to form naturally occurring Silica(SiO2), Alumina(Al2o3) and Aluminosilicate minerals [9][11]. Here, Aluminosilicates refers to materials where aluminum replaces silicon at the tetrahedral co-ordinates within the silica framework, or occupies vacant tetrahedral and/or octahedral sites present in the silicate network sometimes accompanied by the presence of other cations. There has been extensive research and efforts in synthesizing aluminosilicates such as synthetic zeolites [12] , silica modified alumina [9], which have extensive technological and engineering applications that include catalysis, mechanical protection systems and filtration. Aluminosilicates, like many other naturally occurring minerals, have low thermal conductivity. However, they have a much better ability to include pores in their structures. They are abundant in mine tailings, which makes it a very convenient choice for development of a low cost thermal insulation material that can be applied in hot underground mines and building insulations. Furthermore, geopolymers have attracted a lot of interest as a low-carbon footprint alternative that is derived mostly from waste products such as mine tailings. Partially driven by the previous work in creating silica alumina foams by Rao et. al., **Error! Reference source not found.** this thesis is focused on studying more properties of the synthesized foam and devising ways to manufacture it in slightly larger batches to set forth a stage to further develop mass production.

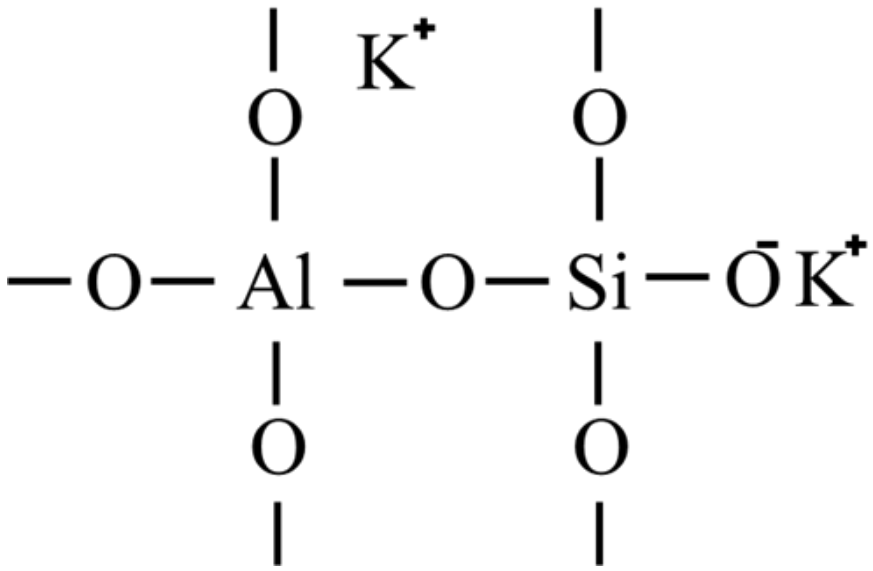

Fig. 4 - A schematic representation of Aluminosilicate Structure

2.2 Porous Aluminosilicates

Porosity has long been the go-to method to reduce thermal conductivity. Air is an excellent thermal insulator and is widely used in various applications. Air trapped within a material's physical structure makes the final product more thermally insulating than just the material itself. House insulations, woolen sweaters, blankets, double-pane windows, all use the exact same principle to be thermally insulating. They all trap air within them and the air does all the work of slowing down heat transfer.

Using the same approach, porosity in aluminosilicates will help make the aluminosilicate more thermally insulating. This thesis will discuss the thermal and mechanical properties of porous aluminosilicates using numerical methods and comparing those with the experimental analysis.

2.3 Thermal conductivity estimation

The measurement of thermal conductivity of a material is not at all easy in a laboratory. There are multiple complications that can arise from factors like insulation, convection and radiation, and human errors, etc. that will cause the results to have compounded errors on them if not done properly. On top of that, such experiments take a lot of time, effort and money to do. Even after spending all that, it cannot be guaranteed to have recorded sufficient error-free data to make any proper conclusions. In comparison to that, numerical methods are a convenient and powerful alternative to laboratory experiments for estimating the thermal conductivity [14]. Using numerical methods can generate massive amounts of data points with much less effort, time and costs to it. Using the detailed and much larger data sets, one can analyze the data and get a good idea in terms of what to look for and how to design the experiments. Using the detailed data points, once we get an approach to take, we can then use experimental analysis to confirm the results we got in the numerical methods. Once confirmed, one can easily conclude the numerical methods to be in line with the experimental results or not. The use of numerical methods to guide the experimental analysis is a widely used method to accelerate the pace of investigation of the study being performed.

There are various types of numerical methods available for thermal conductivity estimation each with its own level of providing detailed results. Molecular dynamics simulation provides with atomic level of details. Boltzmann Transport Equation (BTE) is a meso-scale technique and can serve to bridge atomistic and macro scales. Monte Carlo simulation (MC) can be 'scale-agnostic' depending on the way it is used. Finite Element Method (FEM) is typically applicable to macro scale systems. These methods are very effective when used appropriately. However, lack of understanding of their applicability for various cases can lead to flaws in estimation [15].

Molecular dynamics simulations are very effective in studying the atomic level properties of materials and can provide a time evolution of the system under various conditions. This flexibility to be able to run controlled environment simulations is a huge benefit for research purposes as this helps researchers to fine tune their research in the right direction and confirm their results using the experimental analysis on the correct set of parameters found out using simulations. Molecular Dynamics can provide important insights into phonon driven thermophysical properties such as thermal conductivity of fluids and solids. The accuracy of molecular dynamics simulations is determined by the choice of an appropriate inter-atomic potential, which is necessary to account for the atomic and molecular interactions.

At the macro scale, Finite Element Analysis (FEM) can be used to solve the heat transport equations when the thermonuclear properties of the material constituents is known. The details are discussed further into the thesis.

2.4 Foam synthesis

Rao et. al.**Error! Reference source not found.** used a direct foaming technique to fabricate the aluminosilicate foam of varying porosities by changing the surfactant and blowing agent's concentrations. Alumina powder, silica powder and sodium hydroxide were mixed to form an aluminosilicate slurry. Stearic acid (surfactant) and hydrogen peroxide (blowing agent) were added in the slurry to an appropriate quantity. The slurry is then cured in a convection oven maintained at 100℃ for fix amounts of times to obtain the desired aluminosilicate foam.

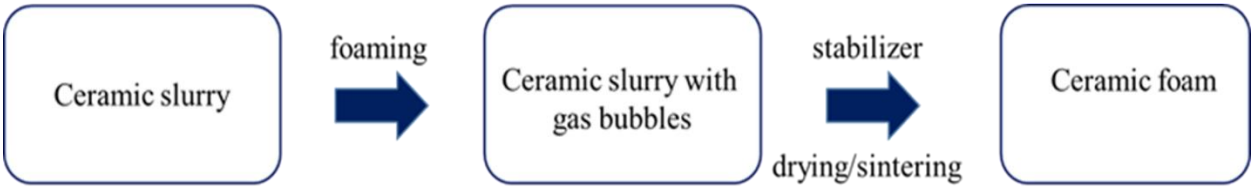

Fig. 5 - Schematic showing the outline of foam making process

The fabrication of aluminosilicates foam requires numerous and time-consuming trial and error cycles of different experimental parameters. To guide experiments, optimize the desired behavior of the foam, and reduce the number of trials, computational methods have been implemented to study the different parameters that govern the foam's thermal and mechanical properties. Molecular dynamics simulations were used to characterize the thermal properties of the aluminosilicate foam at the nanoscale. Finite element analyses were performed to estimate the mechanical properties of aluminosilicate foam at the macroscopic scale.

Different concentrations of Hydrogen Peroxide (Blowing agent) and Stearic acid (Surfactant) were used to study the effects of changing their concentrations on the final foam. A control sample with no Hydrogen Peroxide (HP) or Stearic Acid (SA) had a density of 1.7 g/cc. Another foam with a HP:SA ratio of 4.5 gave a foam with a density of 0.5 g/cc. Another foam with a HP:SA ratio of 8 gave a foam with a density of 0.22 g/cc. (As shown in Fig. 6)

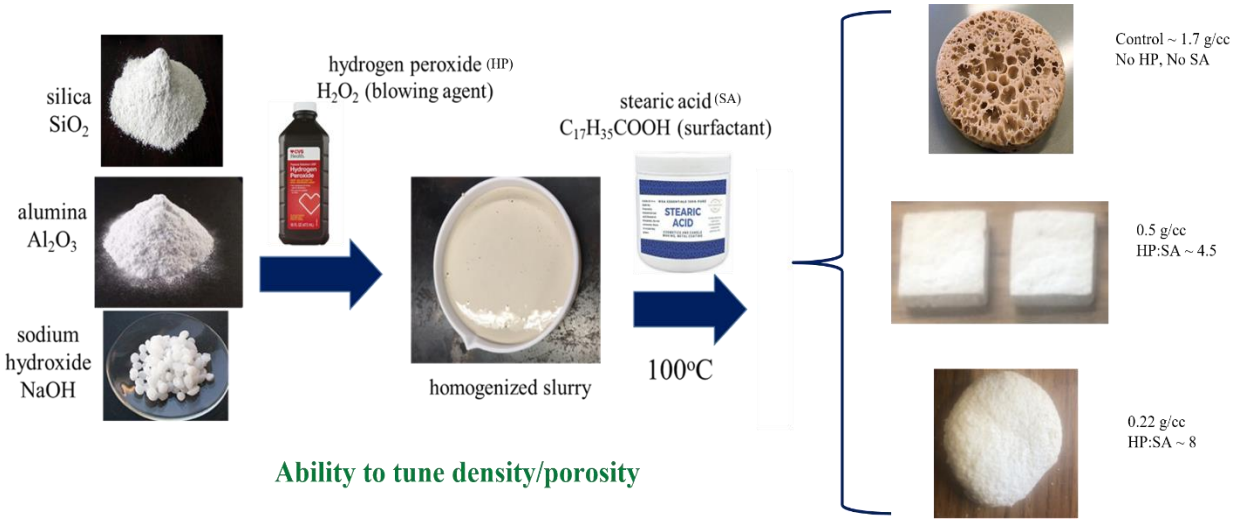

Fig. 6 - Schematic showing ingredients involved in foam making and their results

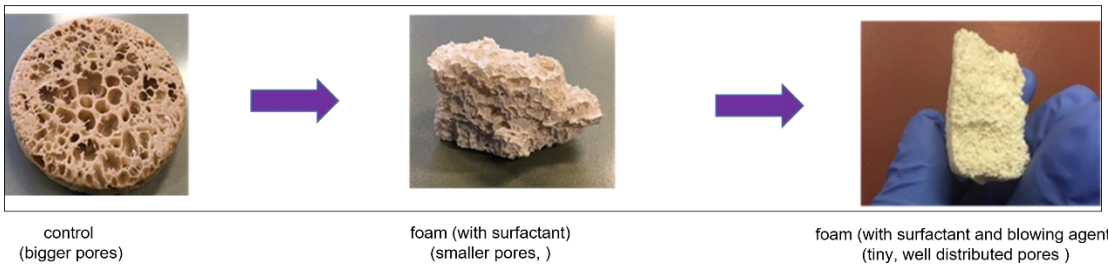

Fig. 7 - Schematic showing comparison between foams with or without HP or SA

Fig 7 shows a side-by-side comparison of effects from changing the composition of Hp and SA. It was noticed that the blowing agent and the surfactant work synergistically to provide a highly porous and stable foam. Just one of the two isn't enough.

Chapter 3: Molecular Dynamics

3.1 Introduction

Thermal conductivity estimations are one of the many applications of molecular dynamics. Molecular dynamics provides a good direction to the design of experiments. There are two ways to estimate thermal conductivity using molecular dynamics viz. Equilibrium and Non-Equilibrium [16]. Equilibrium Molecular Dynamics (EMD) uses Green-Kubo method to estimate thermal conductivity[17]. In contrast, Non-equilibrium Molecular Dynamics (NEMD) method is similar to a laboratory setup of a heat source and a sink [18]. EMD is generally applicable to the homogenous system. Since the PAS structures used in this research are homogenous, EMD is a more suitable option. Green-Kubo formula is a standard relation for thermal conductivity estimations using the EMD method. It integrates a heat current autocorrelation function (HCACF) multiplied with some constants to get the thermal conductivity, as shown in Eq. 1.

$$k = \frac{1}{k_B V T^2} \int_0^\infty \langle q(t).q(0) \rangle \, dt \qquad \textbf{Eq. 1}$$

Here, k is thermal conductivity, kB is Boltzmann constant, V is the volume of the simulation cell, T is the temperature of the equilibrated system, q denotes the heat current in a specific direction, , and the integration $\int_0^\infty \langle q(t).q(0) \rangle \, dt$ refers to the heat current autocorrelation function (HCACF). The Green-Kubo function requires the HCACF to converge to zero to get an accurate thermal conductivity. This, however, theoretically requires an infinite amount of time, which is not possible computationally. A finite time of simulation thus needs to be established that provides acceptable results.

3.2 System Setup

The Porous Aluminosilicate Structure (PAS) consists of Aluminum (Al), Sodium (Na), Oxygen (O) and Silicon (Si) atoms. Different ratios of Si-Al atoms were taken into consideration for study. Molecular Dynamics simulations were performed for Si:Al ratios of 1:1, 2:1, 3:1 and 4:1. All the ratios were studied independently under same system parameters to investigate the variation in thermal conductivity with other parameters like density and porosity. The thermal conductivity was compared to the tensile strength of similar systems (discussed later) to find out the best combination of both, strength and thermal conductivity. Out of the 4 ratios studied, it was found that 3:1 came out to be the best in terms of tensile strength and thermal conductivity.

In total, 44928 of these atoms were initially defined in a cubical unit cell. The numbers of each kind of atoms were based on the stoichiometric ratios and the simulation cell was assumed to have periodic boundary conditions. Here is an example of the system with Si:Al ratio of 3:1 shown in the following table.

Atoms	Mass	Charge	Number of Atoms
Al	26.98	1.8	3241
Na	22.98	0.6	3241
O	16	-1.2	25928
Si	28.065	2.4	9723

Table 2 – Number of atoms, their mass and their charge in the 3:1 Si:Al ratio setting

3.3 Study Parameters

An already equilibrated system was used for all the simulations where all the atoms were at stable locations in the initial system. The aim of these simulations was to understand the effect on thermal conductivity from the following:

1. Optimal Si:Al Ratio in the system

2. Change in Density
3. Inclusion of Pores
4. Vibration characteristic of the phonon
5. Mechanical properties of multiple systems

Now, to understand the effects of Si-Al ratio on the thermal conductivity, simulations were performed at those different ratios and the results were compared. The next part was to understand the effect of density on the system, so in order to achieve this, the size of the unit cell was increased keeping the mass constant. This changed the effective density of the system to study its effects on the thermal conductivity. The next part was to include pores within the system to study the effects of porosity on thermal conductivity, as shown in Fig. 8 below. This was achieved in two ways, one with a central single pore and other with random pores with equivalent volume as the single central pore. The results were then compared to study the difference of both systems.

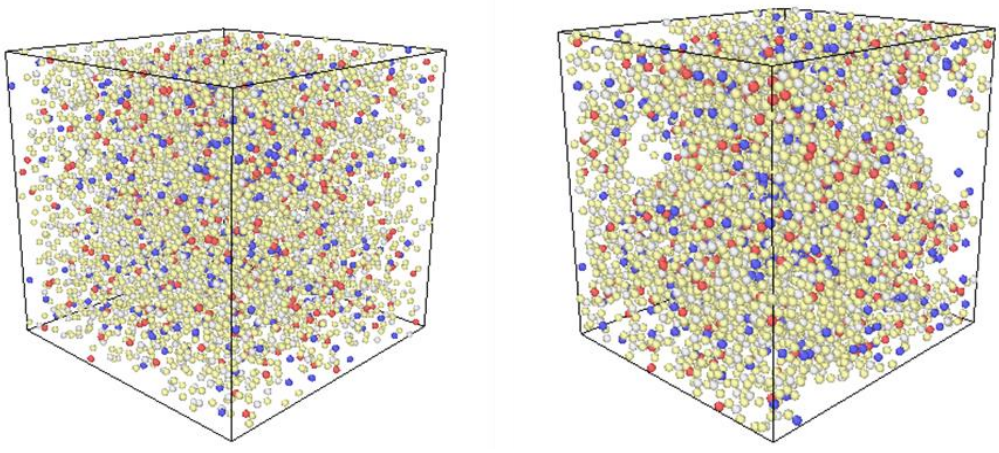

Fig. 8 - Section of a 3-D simulation cell. Left: Simulation cell after blowing up the side length, Right: Atoms in a stable structure after the simulation

The 300K equilibrated structure for a PAS structure with a Si-Al ratio of 3:1 is shown in the Fig 8 above. The corresponding density equaled 2.62 g/cc. The simulation cell size was approximately 83x83x83 $Å^3$

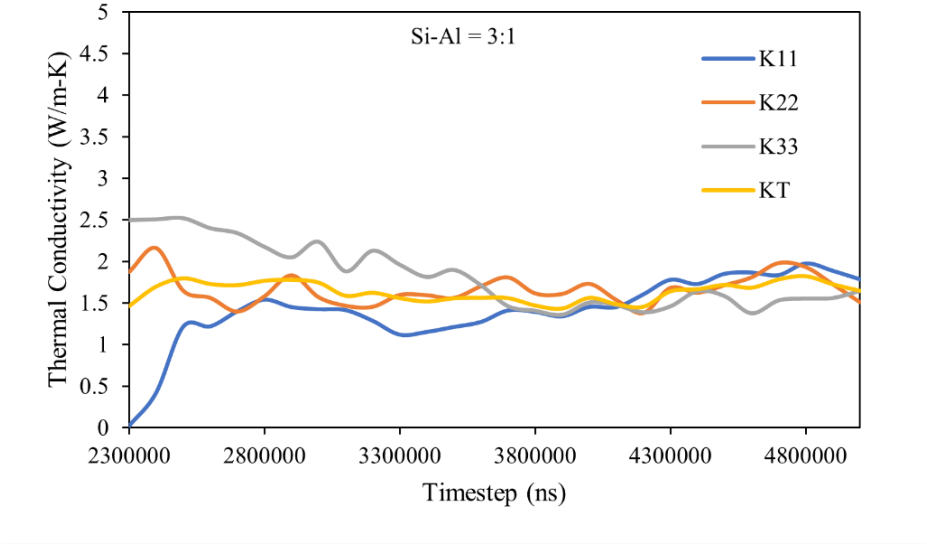

Fig. 9 - A convergence of thermal conductivity from all three-directions for Si-Al ratio of 3:1

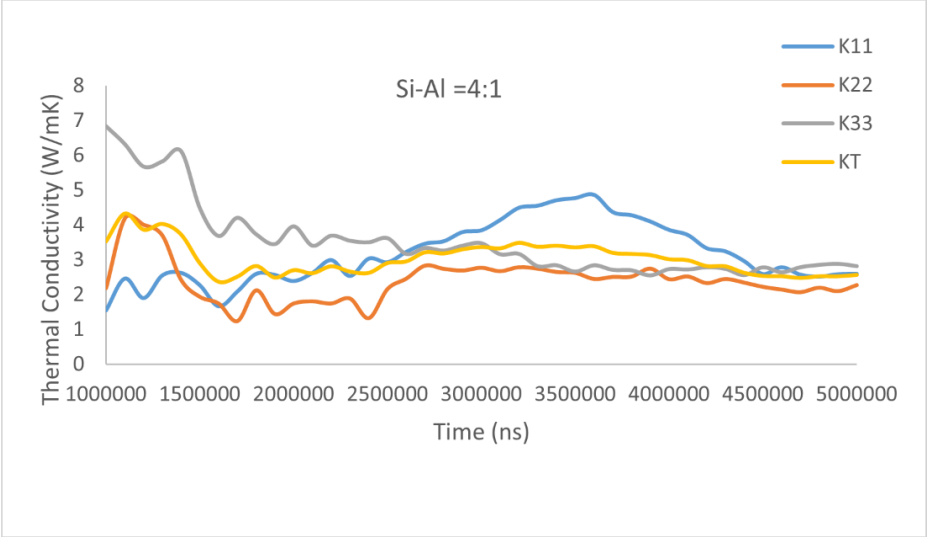

Fig. 10 - A convergence of thermal conductivity from all three directions for Si-Al ratio of 4:1

3.4 Si-Al ratio

Sadat et. al [19] studied the Ultimate Tensile strength (UTS), Young's Modulus (E) and Bulk Modulus (G) at different Si-Al ratios using molecular dynamics simulations as shown in the following figures 11, 12, 13. The data was obtained from [19]. Based on the data presented in the following charts, it is evident, that a Si-Al ratio of 1:1, 2:1 and 3:1 show little change in the Bulk modulus and the Young's modulus and shows a steep decline at the Si-Al ratio of 4:1. Meanwhile, the Si-Al ratio of 2:1 and 3:1 shows higher ultimate tensile strength compared to 1:1 and 4:1 ratios.

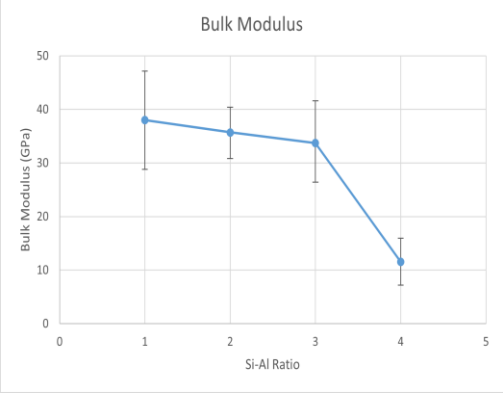

Fig. 11 - Variation of Bulk Modulus with Si-Al ratio [19]

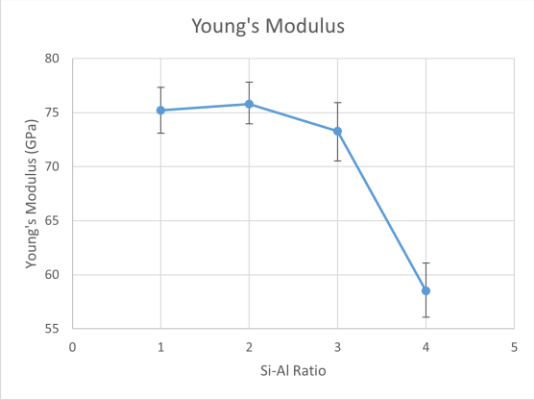

Fig. 12 - Variation of Young's Modulus with Si-Al ratio [19]

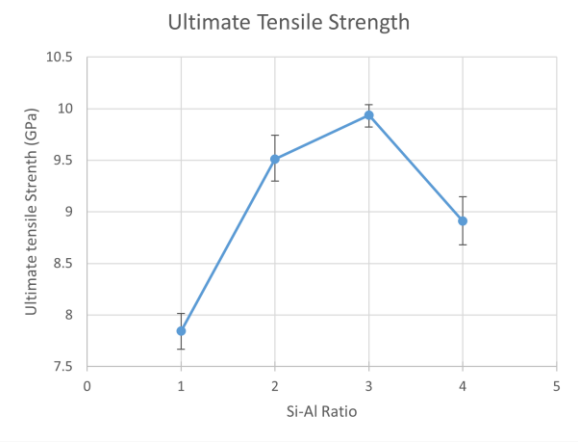

Fig. 13 - Variation of Ultimate Tensile Strength with Si-Al ratio [19]

All 4 ratios of Si-Al were studied to investigate the effect of composition on thermal conductivity of the aluminosilicate geopolymer. The Si-Al ratios of 1:1 and 3:1 were found to have lower thermal conductivity compared to 2:1 and 4:1. The systems were studied for lower densities as well and as expected, the reducing density further lowered the thermal conductivity. Fig 14 shows the normalized thermal conductivity which is the ratio of the actual thermal conductivity to the highest thermal conductivity of the bunch.

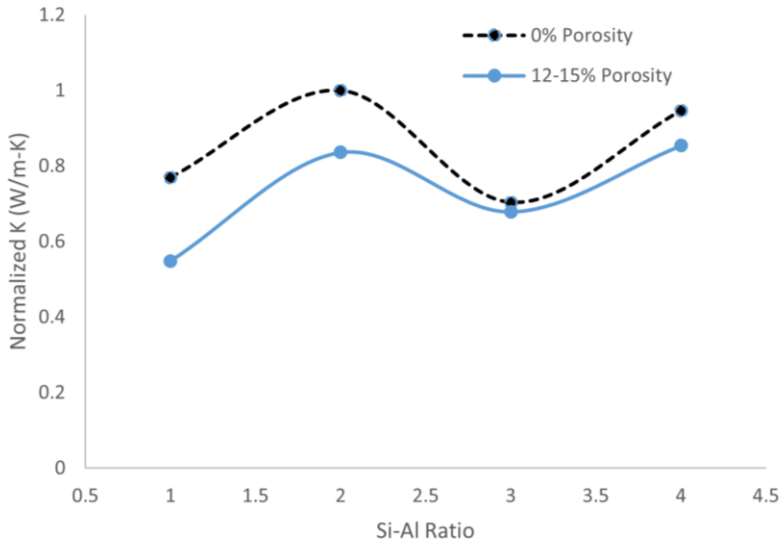

Fig. 14 - Normalized Thermal Conductivity vs. Si to Al ratio for the Aluminosilicate geopolymer system

Comparing all this data to the thermal conductivity data of all ratios, it can be seen that the thermal conductivity for the Si:Al ratio of 3:1 is comparable to that at 1:1 and is lower than that at 2:1 and 4:1. It would be best to go forward with the Si-Al ratio of 3:1 since it has lower thermal conductivity and a higher tensile strength than that for 1:1. Hence, we chose the Si-Al ratio of 3:1 for further detailed studies. The details about thermal conductivity with reducing density has been discussed in further sections.

3.5 Effect of Density

The density of the model was changed by expanding the volume while keeping the mass constant. Molecular Dynamics simulations were carried out for each density to investigate the thermal conductivity. The density was varied from 2.62 g/cc to 0.42 g/cc. The following figure shows the thermal conductivity analysis vs density. Fig 15 shows that with reducing density, the thermal conductivity of the Aluminosilicate Geopolymer is reducing. The figure also depicts a power law that fits the data points.

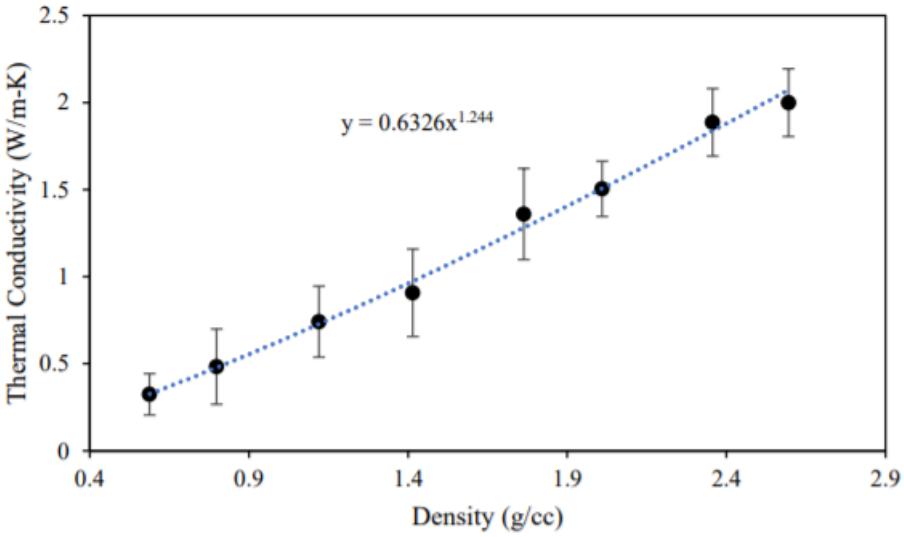

Fig. 15 - Thermal conductivity of porous aluminosilicate structure at Si-Al ratio of 3:1 with density

Densities lower than 0.4 g/cc did not give satisfactory results. The method used involved expanding cell dimensions to lower density and then letting it stabilize. For very low densities, the atoms were too far away to form a stable structure as shown in Fig 16. Thus, the thermal conductivity estimations were not reliable for lower densities.

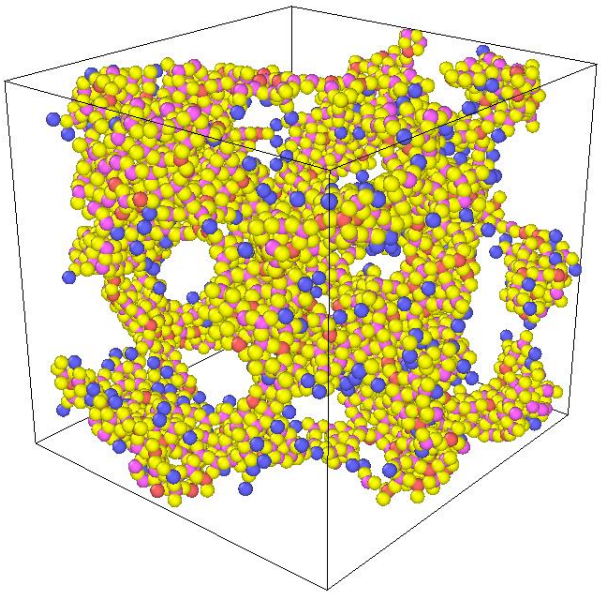

Fig. 16 - Snapshot of the unstable structure after simulation for extremely low densities

3.6 Effect of Pore Distribution

Two different approaches were taken to study the effect of pores on thermal conductivity. Single spherical pore of various sizes was created in the center of the Aluminosilicate Structure and thermal conductivity was measured for those structures. The result in the image below shows that with increasing porosity, the thermal conductivity reduces. This is obvious since a more porous structure will cause more phonon scattering and will in turn reduce the thermal conductivity.

The same porosity structures were tested with random pores of different sizes but the total porosity was maintained in terms of volume removed when compared to its equivalent central pore structure. The thermal conductivity was measured for those systems as well. It was also noticed that the thermal conductivity reduces with increasing porosity which was expected.

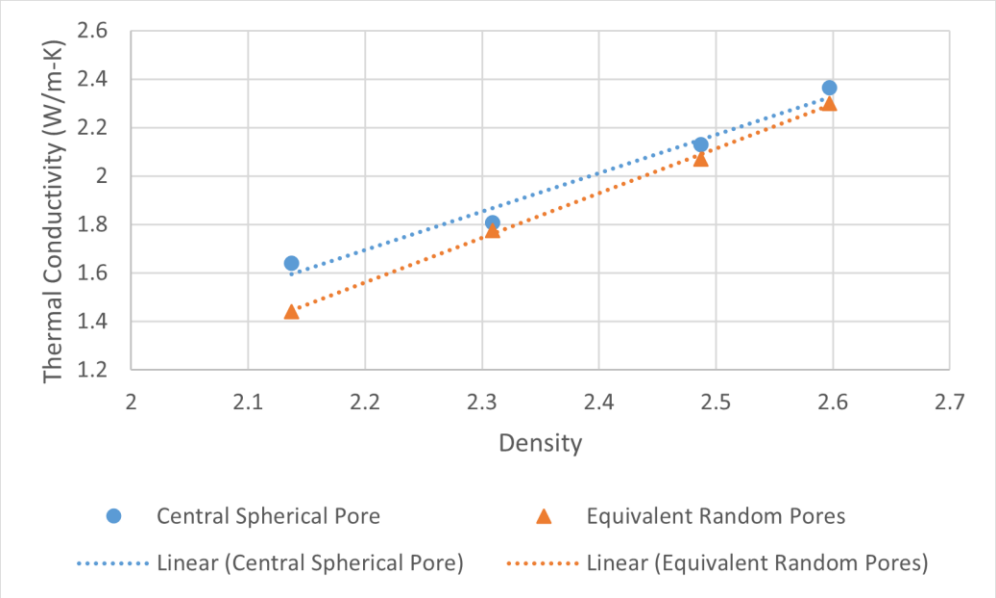

Fig. 17 - Change in thermal conductivity vs. pore sizes and equivalent pore sizes

It was also noticed that for the same porosity, the thermal conductivity for the equivalent random pore structure was slightly lower than that for the central pore structure of same porosity. The reason behind this being, when we split the single pore into multiple smaller pores, even though the porosity remains constant, the surface area of the spheres increases. Due to this increased surface area, the phonon scattering increases. This increased phonon scattering in turn increases the mean free path of the phonons thus reducing the thermal conductivity even more.

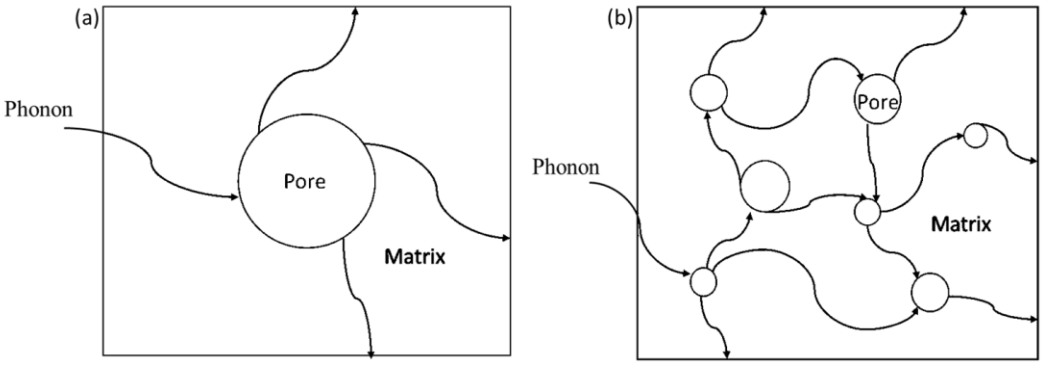

Fig. 18 - Mean free path of the phonon with single and multiple random pores with equivalent porosity

3.7 Study of the vibration characteristics of a phonon

Heat transfer in metals is very different than in non-metals. Heat transfer in solids is due to conduction. Conduction heat transfer is a transfer of heat without bulk transfer of material within the solid and instead, heat is transferred by means of molecular excitement. It happens due to a combination of lattice vibrations of molecules and energy transport by free electrons. In metals, heat is predominantly transferred by the free electrons and in non-metals, vibration transfer is the major method of heat transport [21].

In a dielectric material, heat is essentially carried by vibrations of atoms which are essentially sound waves. At each vibrational frequency, it is dictated by quantum mechanics principles that the vibrational energy must be a multiple of a basic amount of energy, called a quantum. The vibrational energy of those particles is thus quantized into so-called "phonons". Just like photons of light, phonons are virtual particles and the heat that is transferred by these atomic vibrations is referred to as phonon transport. Phonons are not like photons of light, they do not interact between different wavelengths, but rather have very complicated interactions which are referred to as scattering. Phonons will scatter with defects within the material and they interact with phonons of all frequencies around them. This makes studying phonons very complex [20].

Advanced computational tools can help in understanding the phonon behavior at the nano scale. The vibration characteristic of the different types of atoms within the aluminosilicate structure was studied during the thermal conductivity tests. The velocity correlation function was plotted for each type of atom in the porous aluminosilicate structures and then the Fast Fourier Transformation (FFT) was performed on the velocity correlation data to identify if any characteristic frequency of vibration was present in the aluminosilicate structure. The same was

performed on multiple structures for the single central spherical pore and its equivalent volume randomly distributed pores systems. The FFT results are shown in the fig 19 below.

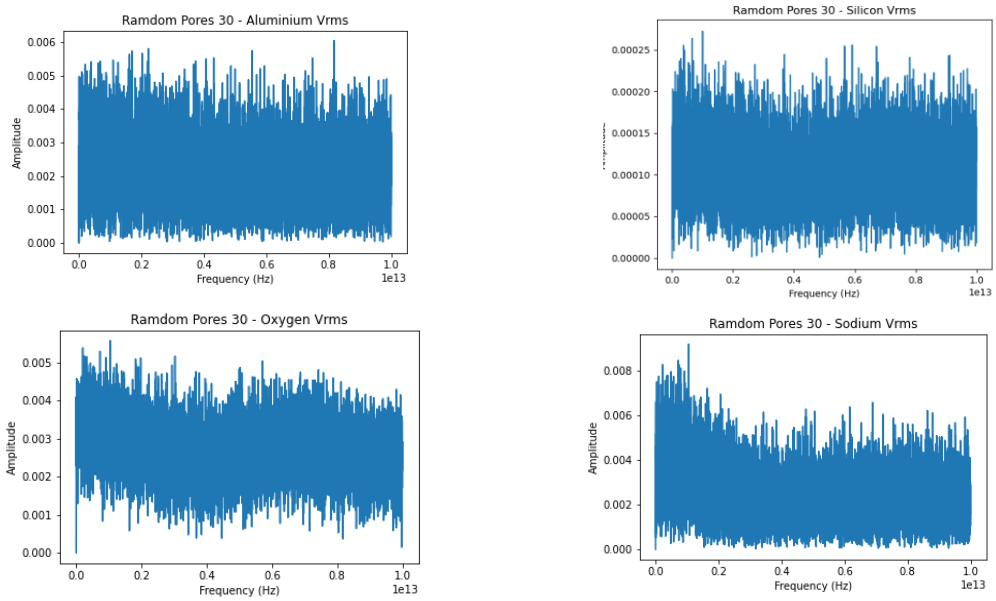

Fig 19. FFT results of all atoms in Random Pores 30 system

When the material is not a conductor, it doesn't have any free electrons in it, so heat is transferred through vibration of the atoms. Now these atoms vibrate in different directions and frequencies depending on the state of energy they are in. These vibrational nodes in the material are called phonons and there is a certain range of frequencies which are typically associated with thermal conductivity.

A perfect and ideal crystalline structure will have infinite thermal conductivity where all the frequencies are propagated without any obstruction but the reason why we never have infinite thermal conductivity is because all these vibrations don't sustain long enough and get dissipated due to imperfections in the structure of the material. And since heat is being conducted in all three directions, there is a scattering effect and different frequencies interact with each other to create hinderance. Now these scattering effects become more pronounced when the vibration encounters different type of atoms, or an impurity, a defect or even an absence of a carrying

medium, that is an empty space like a pore, leading to reduction in thermal conductivity. Also, if the structure is amorphous, this dissipation becomes even more pronounced due to the lack of order in the structure and hence reduces the sustainability of the phonon even more.

Now to test that, we performed velocity autocorrelation function on the system during thermal conductivity simulations to track the vibrational characteristic of an atom through time in relation to itself. It looked at the energy variations of the atoms to find out how the energy variation is correlated to itself after some time. An atom never just participates in a single set of motion and will always have multiple nodes of vibrations on it at any given time. So its velocity autocorrelation is weak.

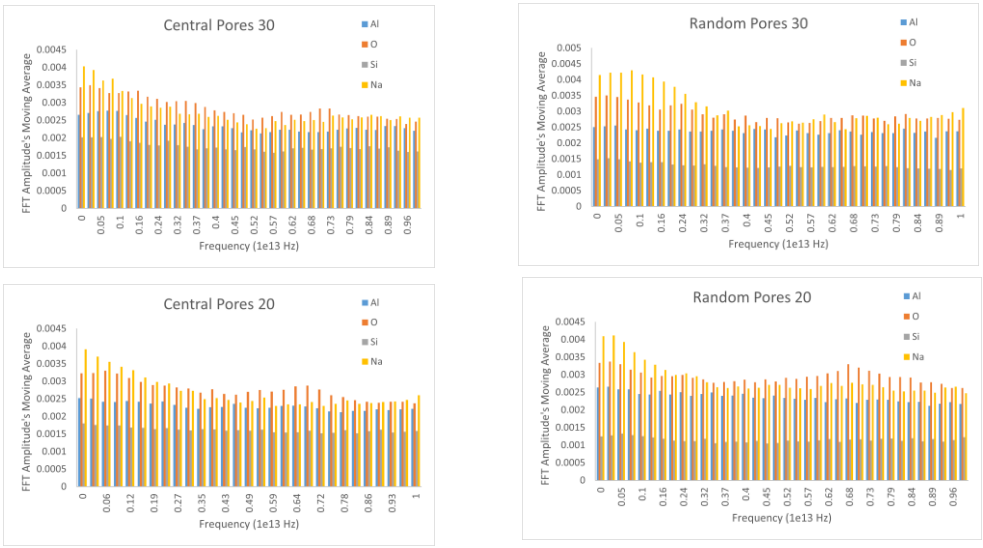

Fig. 20 – Moving average of FFT results

The graphs in Fig 20. show the moving average of the Fourier transformation of the velocity autocorrelation function. This gives us all the nodes of vibrations that that atom is participating in. And clearly, since this is an amorphous system, we will have a bunch of different vibration nodes due to high level of scattering and dissipation in the system. The charts show that there is no frequency dependence on the transfer of a phonon which completely agrees with the amorphous nature of the material.

The system due to its nature of having multiple types of atoms and defects like pores in it was having tremendous effects on the vibration characteristic of the system and hence no specific range of frequency was noticed in the systems. The propagation velocity is a critical factor when it comes to thermal conductivity. The system is too noisy to have a single standard propagation velocity of phonon transfers.

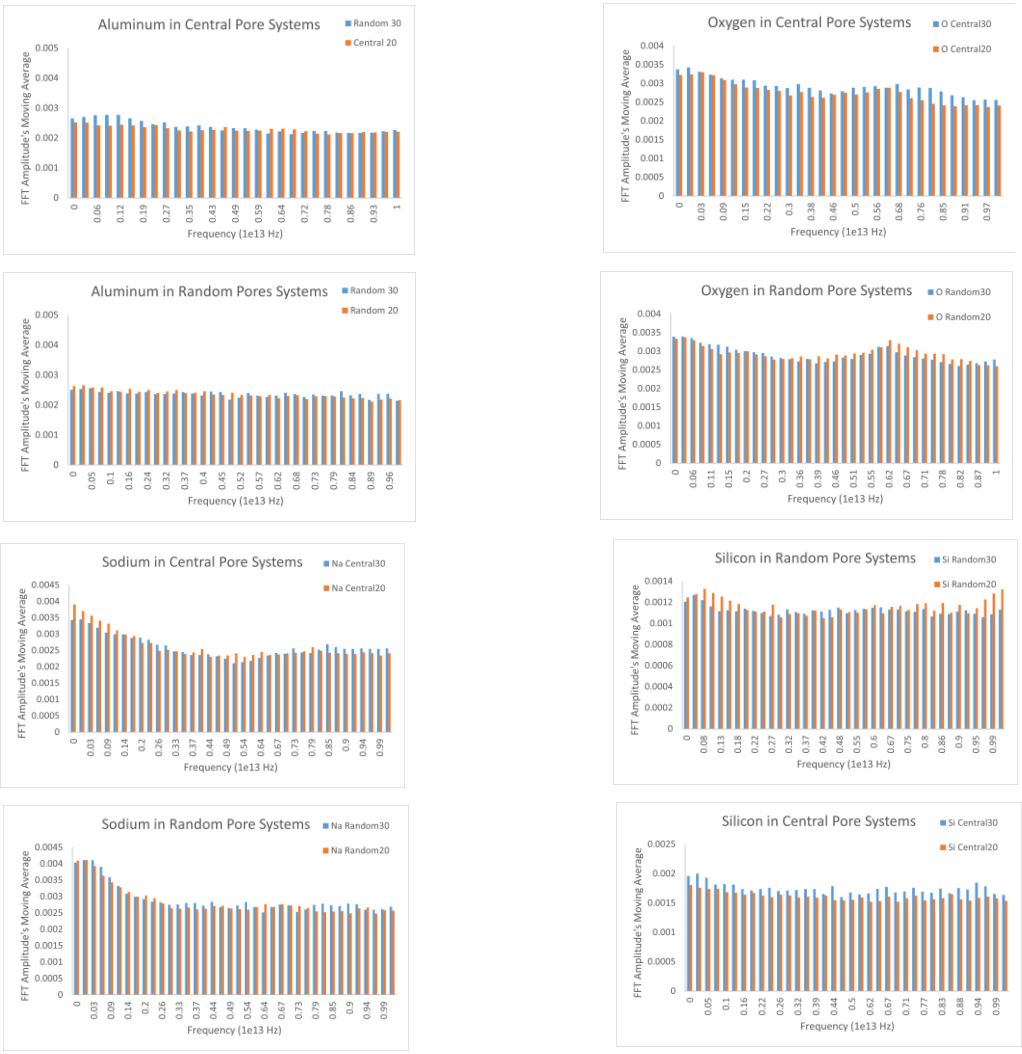

Fig 21. Comparison between FFT curves of same atom in systems with different densities

To study if there is a dependence on FFT as a function of density, we plotted the moving averages of FFT for different density systems. From the graphs in Fig 21, it is observed that the FFT distribution for each type of atom in the central pore 30 system is very similar to that in the

central pore 20 system for both pattern and amplitude. Same was observed with the distribution in the random pore 30 system and the random pores 20 system. Velocity correlation function of all the atoms doesn't seem to be dependent on the porosity or density of the system.

3.8 Measuring mechanical properties using molecular dynamics

The mechanical properties of the porous alumino silicate structure were studied under different porosities. Two different approaches were taken for porosity, central single pore of a particular radius and the equivalent porosity in the form of multiple pores of random sizes. Pore sizes of 5Å, 10Å, 15Å, 20Å, 25Å and 30Å were studied for both its single central pore and equivalent random pores structures.

Both structure formats showed similar trends to porosity and aligned well. The following figures show the relation of density to its Bulk Modulus, Shear Modulus, Poisson's Ratio, Young's Modulus. It is noticed that the Bulk modulus and shear modulus reduce with increasing porosity. The Young's Modulus also shows similar trend to increasing porosity.

Since the simulation box remains the same, increasing porosity causes reduction in density.

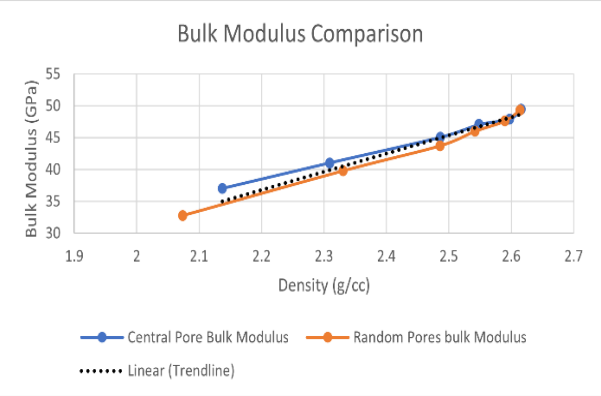

Fig. 22 - Bulk Modulus vs Density

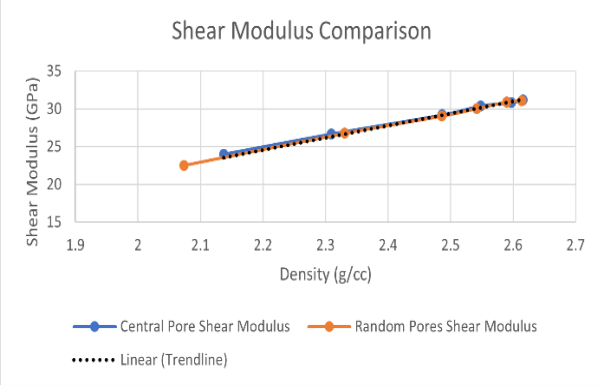

Fig. 23 - Shear Modulus vs Density

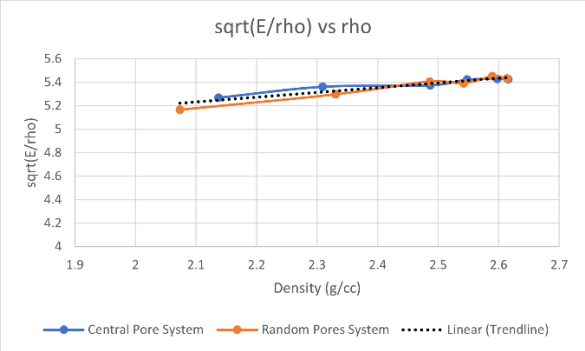

Fig. 24 - Young's Modulus vs Density

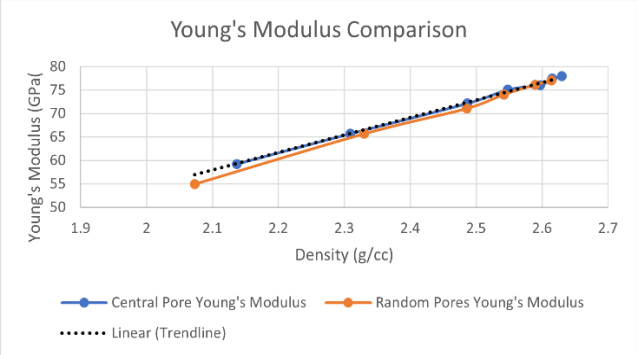

Fig. 25 - Sqrt (Young's Modulus/Density) vs Density

The vibrational characteristic of a material is highly co-related to the speed of sound in that material. That's because, heat is generally carried by the high frequency vibrations. And even though all the high frequency vibrations may not be travelling at the speed of sound, it is still a good approximation to go with. It is a well-accepted phenomenological model that all these nodes of phonon that are carrying heat move at the speed of sound. The speed of sound goes by square root of young's modulus over rho. The speed of sound seems to be dependent with the change in porosity. It is present even though its not very prominent. As seen in Fig. 24, the velocity of sound reduces with increase in porosity i.e. decrease in density.

It was observed that the Young's modulus reduces with density. Young's modulus is depended on the stiffness of the bonds, so the more defects we put into the system through pores the weaker will be the bonds that are closer to the defect.

We performed all these simulations on two types of systems for a given density, one with a single central pore and one with the equivalent distribution of random pores. This was done to study the effects of pore size distribution and whether or not smaller pore size will be better than the bigger pore size. Just like the thermal conductivity reduces with smaller random sized distributed pores. The mechanical properties also reduce with the random distribution of smaller

pores when compared to the equivalent central single pore system. The reduction in thermal conductivity from central pore to random small pores can be traced back to the velocity dependence of the system.

So, having wide distribution of smaller sized pores will have lower thermal conductivity than the equivalent bigger pore counterpart. And since our aim is to have lower thermal conductivity, we need to reduce the density and as well as reduce the pore sizes that contribute to that same density.

$$\kappa = \frac{1}{3} C_P^V V_S \lambda$$

-Eq. 2

From Eq. 2, where K is the thermal conductivity and Vs is the longitudinal speed of sound

Its evident that thermal conductivity is directly proportional to the speed of sound in the medium along with Volumetric heat capacity and the effective phonon mean free path.

Chapter 4: Acoustic Analysis

4.1 Introduction

The measurement of mechanical and thermal properties of highly porous foams is not always feasible due to the brittleness of the samples and/or the capability of available instruments. In such situations, when direct measurement of physical properties is problematic, numerical modeling provides a practical alternative. Numerical simulations could be used to guide experiments and reduce the number of trial-and-error cycles necessary to optimize the design and fabrication of materials. In this study, Finite Element modeling was conducted to examine the relationship between the acoustic and elastic properties of the foam and the effective density at macroscopic scale. The mechanical properties data for the solid matrix of the foam were obtained from molecular dynamic simulations conducted by Sadat et. al [19] and are shown in Table 3. The Structural Mechanics module from COMSOL Multiphysics was used to perform the macroscopic simulations. Isolated symmetrical spherical pores were inserted in the model to represent porosity. Since the pores are assumed to be filled with air, the stiffness of air was considered to be negligible. The modeling, therefore, provided the effective elastic properties of the foam. Acoustic simulation was conducted to estimate the longitudinal wave (P-wave) velocity and shear wave (S-wave) velocity. Elastic properties were then derived using the relationship between P-wave velocity, S-wave velocity, and the density of the materials. The relationships are as shown in Eq. 3 through Eq. 6

$$v_P = \sqrt{\frac{K + \frac{4}{3}G}{\rho_{eff}}} \qquad \textbf{Eq. 3}$$

$$v_s = \sqrt{\frac{G}{\rho_{eff}}} \qquad \textbf{Eq. 4}$$

$$K = \frac{E}{3(1-2\nu)} \qquad \textbf{Eq. 5}$$

$$G = \frac{E}{2(1+\nu)} \qquad \textbf{Eq. 6}$$

Here v_P is P-wave velocity, v_s is S-wave velocity, K is bulk modulus, G is shear modulus, ρ_{eff} is effective density, E is Youngs modulus.

Young's Modulus (GPa)	Density (Kg/m^3)	Poisson Ratio
75	2620	0.25

Table 3 - Solid Matrix properties fetch from MD simulation

We also performed stress analysis to get the elastic constants and then used the Eq. 3 to 6 to estimate the P-wave and S-wave velocity.

4.2 Acoustic Simulations

A solid matrix model of 4x4x4 cm^3 was created in COMSOL. The mechanical properties of the solid matrix were fetched from Table 3. Modeling is done based on the wave theory and similarity principle [22]. Symmetric pores of different sizes were created inside the solid matrix to get different porosities as shown in the Fig. 226. The porosity and effective density are calculated using Eq. 7 and Eq. 8.

$$\phi = \frac{v_t - v_{pr}}{v_t} \qquad \textbf{Eq. 7}$$

$$\rho_{eff} = \frac{\rho v_p}{v_t} \qquad \textbf{Eq. 8}$$

Here ϕ is porosity, v_t is total volume, v_{pr} is pore volume, ρ_{eff} is effective density, ρ is the solid matrix density.

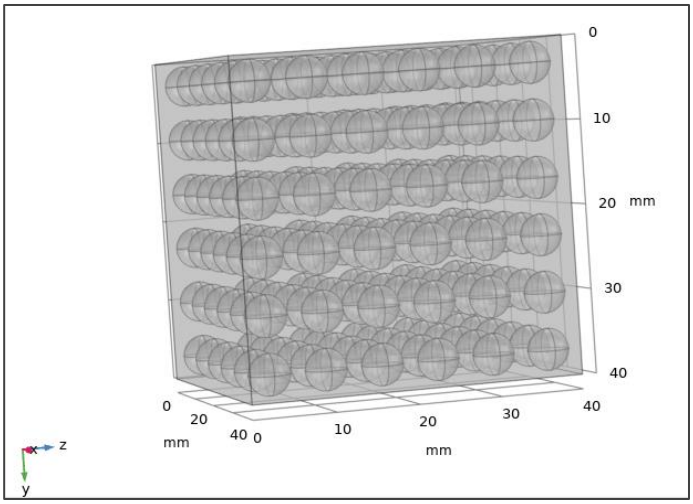

Fig. 16 - 3D symmetric model

The model is assumed to be isotropic, homogenous, and linear elastic material. Elastic Solid Mechanics module is used to define the boundary condition and wave pulse excitation on the face. The transducer excites one surface of the model by a force pulse, namely, the force is applied at the bottom edge, and the displacements were monitored with passage of time at the opposite end. The piecewise function tool was used to generate a time dependent sinusoidal force wave function of constant amplitude as defined by the Eq. 9. The pulse is shown in Fig. 27.

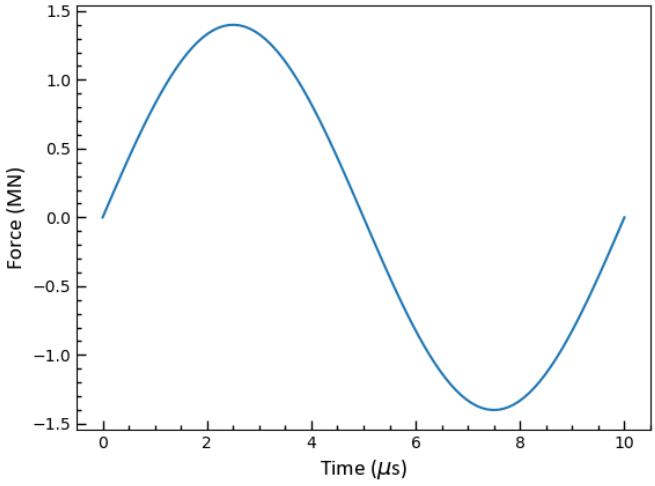

Fig. 27 - Piecewise sinusoidal wave

$$P_{(t)} = P_0 \sin(2\pi f_0 t) \qquad \textbf{Eq. 9}$$

Here $P_{(t)}$ is time dependent force wave function, P_0 is Amplitude in N (1.46 MN), f_0 is Frequency (0.1Mhz).

To calculate the P-wave velocity, the excitation was done using the force wave function in the Z-direction. The other faces of the model are assigned to Low Reflecting Surface to avoid any reflected wave at the receiver point as shown in Fig. 28. The boundary of the pores is assumed free elastic boundaries to account for the air. Time dependent study was done for about 2*time-period for both P wave excitation and S wave excitation. The timestep is chosen to be 1/75 times of time-period to obtain sufficient data points leading to better plot in terms of fit/smoothness. Z-displacement was plotted with time at the excitation end point (3) and at the receiver end point (4) which are 40mm apart in the Z-direction as shown in Fig. 28. Same approach was taken for the S-wave velocity calculation. Here the excitation is done in X or Y direction on the same face as the P wave excitation was done as shown in Fig 28.

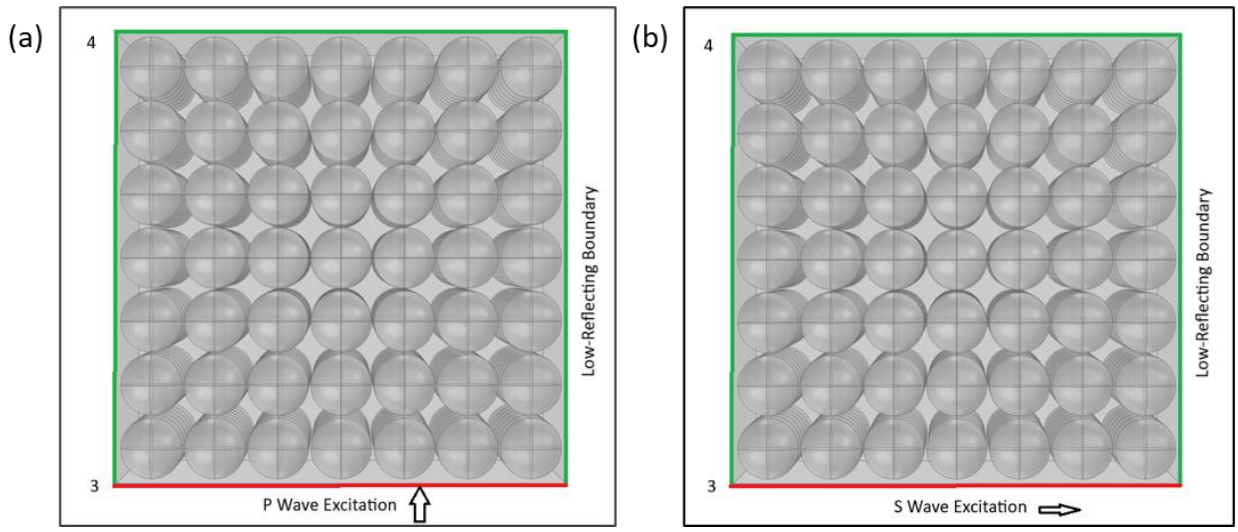

Fig. 28 - (Left) P wave excitation (Right) S-wave excitation

Time phase difference was calculated from the graph from the Z-displacement for point 3 and 4. From Fig. 29. , Vp=40mm/ (13.8-5.4)us= 4761m/s and Vs=3389m/s. Eq. 5 and Eq. 6 were used to calculate the bulk modulus and shear modulus. Youngs modulus was calculated using the Eq. 2 and Eq. 3. This technique was used at different porosities to calculate the elastic properties.

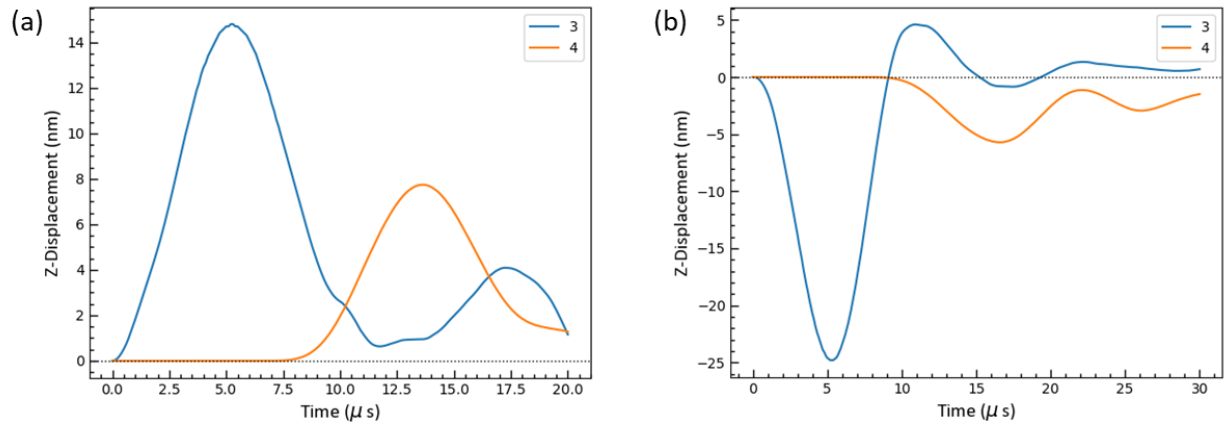

Fig. 29 - (Left) displacement curve for P wave (Right) displacement curve for S wave

4.3 Stress Analysis

A similar model was created for the acoustic simulation. Again, the solid matrix properties were taken from Table 3. The Solid Mechanics module was used to provide the boundary and the uniaxial loading conditions. Force per unit area under elastic limit was applied on one surface of the model in the z-direction while the opposite surface was kept fixed as shown in Fig. 30. The lateral four interfaces were set to be free. Again, the model was assumed to be isotropic, homogenous, and linear elastic material, and so that the elastic moduli are the same in each of the principal direction. We ran a steady state simulation in order to obtain the stress distribution and z-displacement distribution on the model. The average Von-Mises stress and z-displacement were calculated on the applied surface. Strain was calculated using the Eq. 10.

$$\varepsilon = \frac{\Delta L}{L} \qquad \textbf{Eq. 10}$$

Here $\boldsymbol{\varepsilon}$ is strain, $\boldsymbol{\Delta L}$ is the displacement in z direction and $\boldsymbol{L}$ is the total length of the model in z direction.

Youngs modulus was calculated using linear elastic **Error! Reference source not found.**11

$$\boldsymbol{\sigma = E\varepsilon} \qquad \textbf{Eq. 11}$$

Here $\boldsymbol{\sigma}$ is average surface stress, $\boldsymbol{\varepsilon}$ is average strain, and $\boldsymbol{E}$ is young's modulus.

Lateral displacement was also calculated either in x or y direction to calculate the effective Poisson ratio. Eq. 12 was used to get the Poisson ratio.

$$\boldsymbol{\nu = \frac{-\varepsilon_{lateral}}{\varepsilon_{longitudinal}}} \qquad \textbf{Eq. 12}$$

Here $\boldsymbol{\nu}$ is effective Poisson ratio.

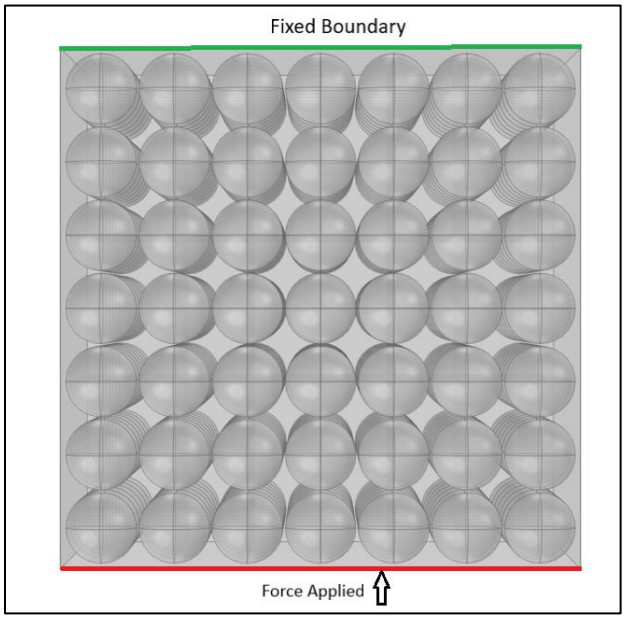

Fig. 30 - Force applied in Z-direction for the stress analysis

The other moduli such as bulk and shear was calculated using the relationship between E and v from the Eq. 5 Eq. 6. P-wave velocity and s-wave velocity was also calculated using Eq. 3 Eq. 4. The simulation was done for different porosities and all the parameters were calculated after each simulation.

4.4 Experimental Analysis

The initial trials involving control samples yielded experimental validation in terms of setup, test variables, optimal specimen dimensions. The results were also verified from data published in the literature. Table 4 includes experimental details for different material types and dynamic properties obtained from ultrasonic tests.

The aluminosilicate system under observation is triphasic, that is, it has a solid ceramic matrix (consisting of aluminosilicate binder as well as precursors of SiO2 and Al2O3), has air-filled pores (due to the evaporation of water because of condensation reactions and hydrogen peroxide decomposition) and also contains adsorbed molecular water which is not entirely eliminated from the final product at low curing (100℃) temperature used in our process of fabrication.

Material Type	Experimental Density	Literature Density	P Wave Velocity	S wave velocity	Experimental Young's Modulus	Literature Young's Modulus
	(g/cm3)	(g/cm3)	(m/s)	(m/s)	(GPa)	(GPa)
Brass	8.64	8.73	4216.4	2235.2	112	97
Aluminum	2.71	2.7	6578.6	3149.6	72.8	71
Copper	9.1	8.96	4851.4	2133.6	111.1	110
Glass (Pyrex)	2.2	2.23	5613.4	3454.4	61.4	64
Sandstone	2.25	2.2-2.8	2946.4	1828.8	17.7	10-20
Granite	2.29	2.6-2.7	6121.4	3784.6	77	20-50

Table 4 – Experimental details for various material types and dynamic properties obtained from ultrasonic tests

The effective concentration of these constituents varies with density and is manifested in the variation of longitudinal velocity (Vp) of the foam under observation. For the same reasons, the Young's modulus of foams decreases with increasing porosity. This can also be attributed to the presence of anomalies and heterogeneities in the form of voids and cracks in low density foams compared to the control samples.

4.5 Numerical Modelling

Numerical modeling was performed to estimate acoustic and elastic properties of the aluminosilicate foam at various densities. The densities were controlled based on the inclusion of pores in the system while keeping the volume constant. The density decreases as we increase the porosity in the system.

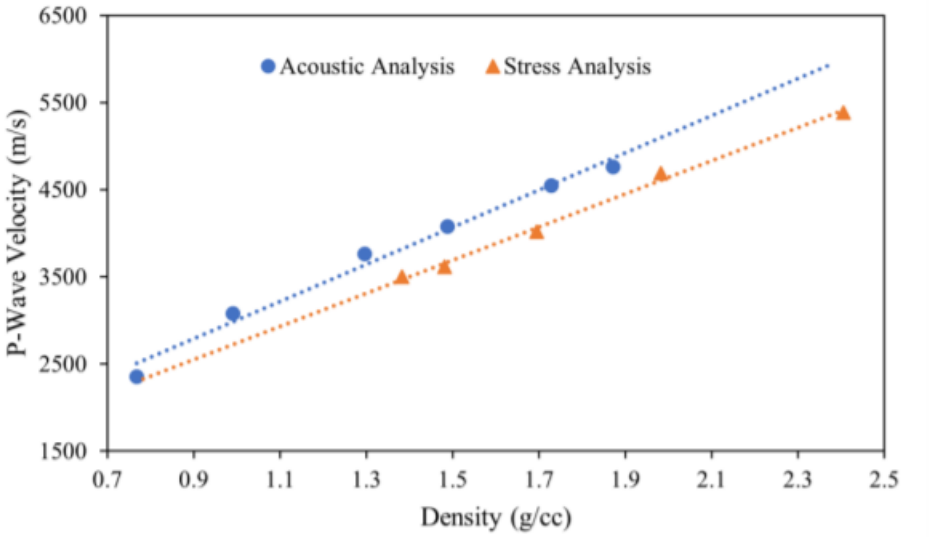

Fig. 31 - Variation of P-Wave velocity with the density for acoustic and stress analysis

Fig 31 shows the correlation of P-wave velocity for both acoustic simulation and stress simulations as a function of density (i.e. with the porosity). The plot reveals a linear trend for P-wave velocity decreases as density decreases. This is attributed to enhanced phonon scattering since as we increase the number of pores, phonons take a longer time to travel through the system. The acoustic and stress simulation data are in good agreement and corroborate the assumption regarding the reduction of the mean-free path for phonon scattering.

Fig 32 shows the variation of Young's modulus with the effective density for both acoustic and stress data. The Young's modulus decreases as we increase the porosity and exhibits a power-law trendline. We ran acoustic simulations on the 3D reconstructed foam in COMSOL to obtain the P-wave and S-wave velocities. The time of flight for P-wave and S-wave velocity was calculated from the maximum Z-Displacement curve, as shown in Fig. 33.

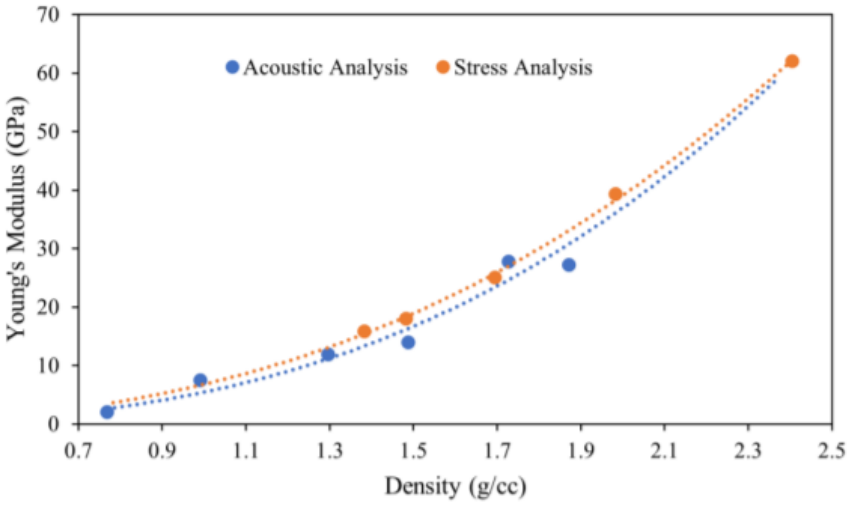

Fig. 32 - Variation of Young's modulus with the density for acoustic and stress analysis

The estimated P-wave velocity is equal to 1857m/s, and the S-wave velocity is equal to 1350m/s, which are very close to experimental results. This methodology was not used for all low-density foams since the mesh generated by Simpleware Software is very fine, and therefore the time and the memory requirements to carry out the calculations are enormous.

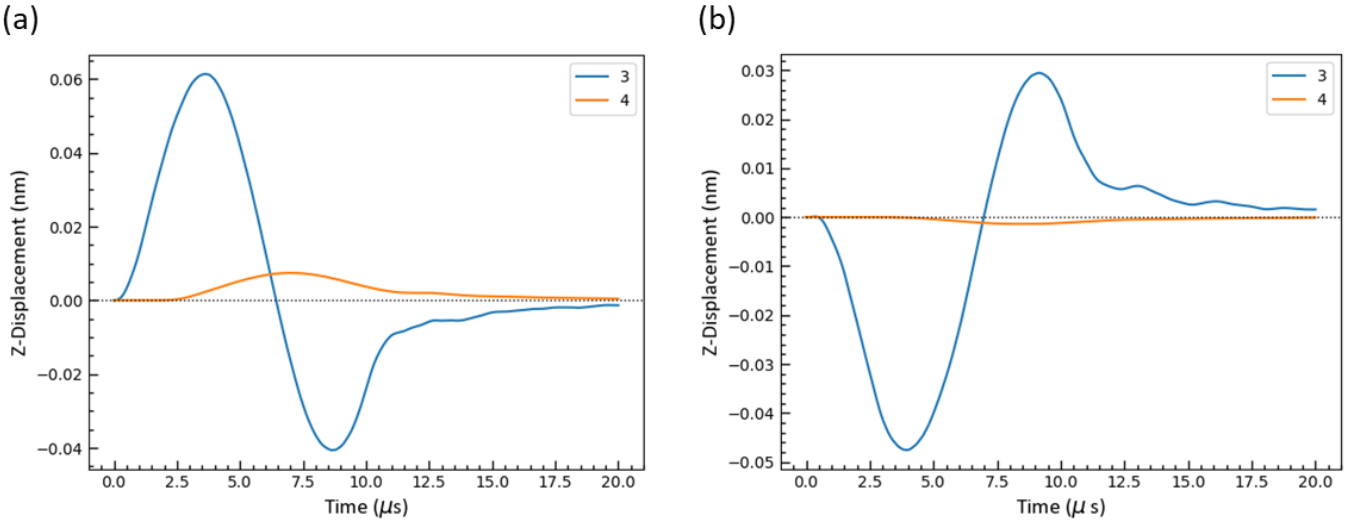

Fig. 33 - (a) Z-Displacement curve for P-Wave excitation used to calculate P-wave velocity (b) Z-Displacement curve for S-wave excitation used to calculate S-Wave velocity

4.6 Estimation of a suitable model

The estimates of the sample porosities are approximate as the pores are not distributed uniformly on the surface and in the interior of the specimens. This may lead to errors in calculation of densities. However, conducting 5 measurements along each dimension (radius/height) would minimize the error to within 1% compared to liquid displacement porosimetry methods. Sample cubes with parallel and flat surfaces were prepared to the best of the author's abilities. Flat and parallel surfaces are essential to ensure accurate measurement of the sample dimensions are carried out and adequate contact between the surface and the source/receiver transducers ends is obtained. Petroleum gel was applied to enhance the transmission of ultrasonic wave energy. However, even a small amount of pressure applied to ensure a good contact between the sample interface and transducers is typically too large and results in cracking low-density samples (Density < 0.28 g/cc). In these situations, conducting numerical simulations aid in the understanding of porosity and sound velocity relationships. The Vp/Vs ratio has been taken to be 1.62 based on several measurements conducted in laboratory. Microstructure and chemistry were not taken into account in our simulations. This also explains the small discrepancy between experimental and numerical modeling results. However, for the purpose of this study, numerical modeling data agree well with experimental data as shown in Fig. 34 and Fig. 35.

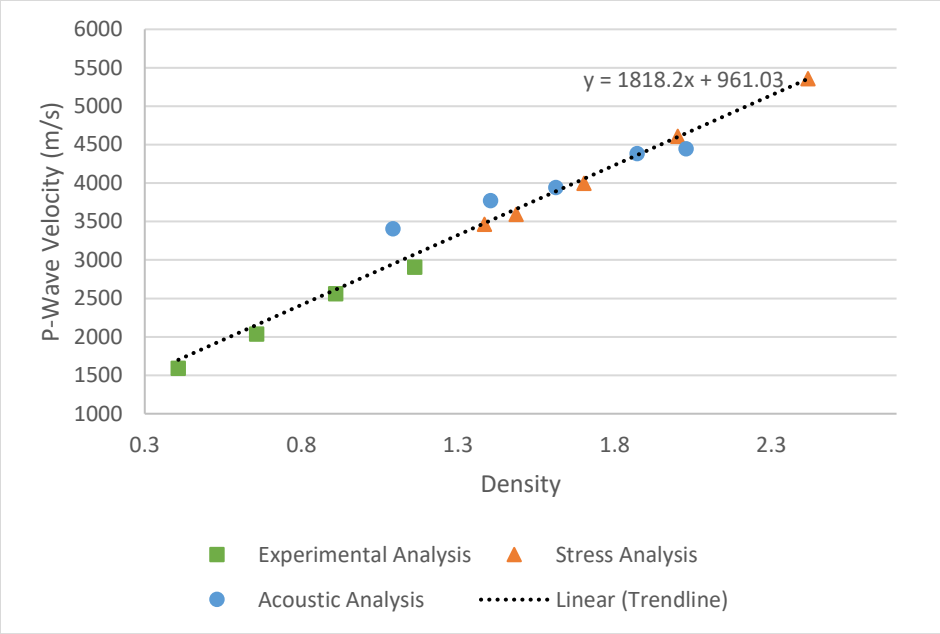

Fig. 34 - P-wave velocity varying with the density of the foam for both numerical and experimental analysis

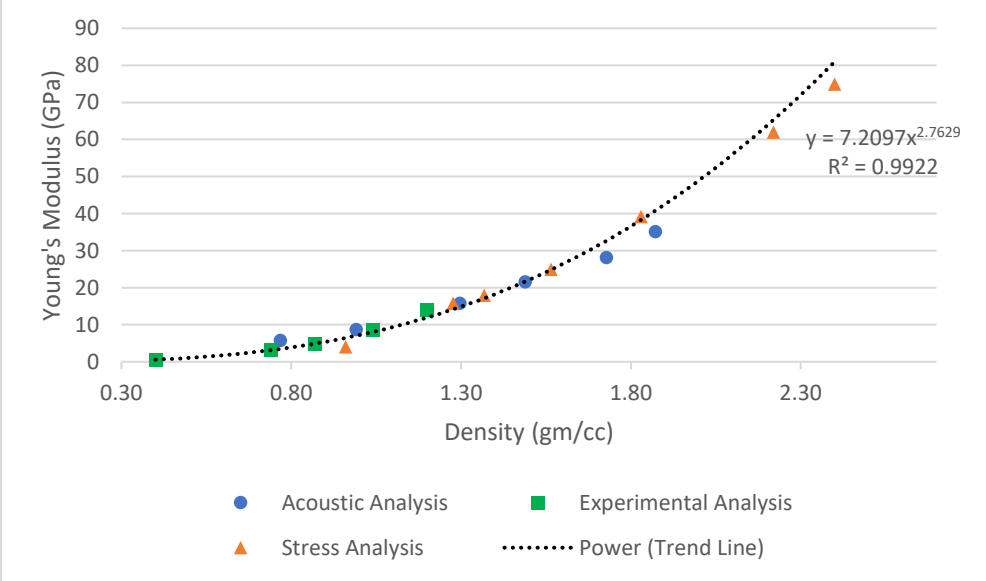

Fig. 35 - Young's Modulus varying with density of the foam for both numerical and experimental analysis

Fig 34. shows a graph of the P-wave velocity versus density for the experimental, acoustic and stress analysis. P-wave velocities are extrapolated for the lower densities based on numerical modeling results and using a power-law relationship. As seen from the figure, the P-wave velocity from each method is very close to each other. Therefore, an estimated model using a

regression line was generated using the average of P-wave velocities in different density ranges and is shown in Eq. 13

$$v_P = 1818.2\rho_{eff} + 961.03 \quad \textbf{Eq. 13}$$

Here v_P is P-wave velocity, ρ_{eff} is the effective density.

A similar approach was taken to develop a model to estimate the elastic modulus. A power-law model was generated for the Young's modulus for a given density as shown in Eq. 14

$$E = 7.2097\rho_{eff}^{2.7629} \quad \textbf{Eq. 14}$$

Here E is Young's Modulus, ρ_{eff} is the effective density.

Chapter 5: Conclusion

Molecular Dynamics is an effective tool to study the thermal behavior of materials with atomic behavior and detail. It serves as a great tool to reduce experimental analysis and focus on optimizing the overall research process and get to the conclusions faster and in a less expensive manner.

Molecular dynamics can study not only different systems but also different conditions within the system. This gives us even more tools to properly study multiple conditions and its effects on the overall system at ease.

While Molecular dynamics might be a great tool to study the effects at nano scale, Finite Element Method analysis serves to be an equally useful tool to study the conditions at a macro scale. It also serves the same purpose as molecular dynamics simulations by reducing the number of experimental analysis and helping focus the energy and time in studying the right configurations more thoroughly.

After having a good understanding of the behavior of the porous aluminosilicate structure from the molecular dynamics and finite element analysis simulations a novel experimental setup was also devised to confirm the simulation results with real world experimental analysis.

Aluminosilicates from the mine tailings can be recycled into a useful foam for use as an insulator. Recycling the tailings also helps cut down on the environmental footprint of the mine. Aluminosilicate is a worthy contender for a cheap and good insulating agent for deep underground mines.

5.1 Molecular Dynamics

Molecular dynamics simulations suggest that the Si to Al ratio of 3:1 is optimum for both lower thermal conductivity and high mechanical strength of the aluminosilicate system studied in this research project. Hence the Si-Al ratio of 3:1 was retained in all other studies. For a density range of 2.62 g/cc to 0.42 g/cc, it was observed that the thermal conductivity decreases with decreasing density, following a power-law regime. The thermal conductivities calculated from

MD data agree well with the experimental measurements for a density range between 0.42 g/cc and 1.7 g/cc, however, MD simulations did not provide suitable results for densities less than 0.4 g/cc. Thermal conductivity values show a linear relationship with the amount of porosity introduced in the sample. It was also observed that random pores embedded in the model provide lower thermal conductivity compared to an equivalent single pore (same porosity) due to more efficient phonon scattering. The vibration characteristics of the phonons were studied and no single frequency of vibration was found to be dominant throughout the system. The mechanical properties of the structure was also studied using molecular dynamics and it shows that the Young's modulus of the structure decreases with decrease in density.

5.2 Acoustic Analysis

The numerical and experimental elastic properties data for the amorphous porous aluminosilicate foam follow a power-law relationship and decrease with increasing porosity. The ultrasound technique provides the opportunity to determine the acoustic properties of a material non-destructively and in a short period of time. The PAS foams' properties vary noticeably from sample to sample for the same density due to the amount of water adsorption in the solid matrix during curing, generation of macro cracks, and errors introduced while measuring the densities. It was observed that the compressional and shear wave velocities decrease linearly with an increase in porosity in both experimental and numerical experiments. Acoustic and elastic properties obtained from experimental and numerical analysis show a high degree of correlation. For that reason, an estimated model was produced by taking the average of numerical and experimental data for the P-wave velocity and Young's modulus.

Chapter 6: Future Work

The results from experimental and numerical analysis show good agreement with each other. However, few assumptions were taken into account to perform the analyses. More research is needed to minimize the variability.

- Continue working on the method of fabricating the foam to replicate the original foam with new set of equipment (Bath and Probe sonicators) to be able to generate the foam in larger batches
- Study the variation of these thermal properties in the larger batch size foams to confirm its consistency with small batch creations
- Continue work on generating the foam using actual mine tailings as opposed to pristine materials
- Composite materials like graphene and fibers can be added to the foam to enhance its mechanical properties
- A hydrophobic coating can be applied to the foam after curing to prevent excessive moisture adsorption
- Measure the thermal conductivity of the foam using the Thermtest TPS 500S system and check its consistency with experimental data.

APPENDIX A – FOAM SYNTHESIS

Recreating Al-Si foam synthesis for Thermal Characterization

Objective: Synthesis of 0.22 g/cc Al-Si foams with Branson bath sonicator

Materials/chemicals:

Quartz or silicon (IV) oxide (SiO_2), 13024 from lot# N06F034 of size < 10 microns and > 99.5 % purity and alpha-corundum or alumina (Al_2O_3), 12553 from lot# Q06C050 >99% purity was used as silicon and aluminum sources as received from Alfa Aesar. Sodium hydroxide (NaOH) pellets A16037, lot# 10213360 as obtained from Alfa Aesar was used to prepare alkali solutions. Ethanol (EtOH) 70% SDA lot #VXB172 was purchased from Volu-sol . *Hydrogen peroxide (H_2O_2 3 wt.%)* Ethyl alcohol (C_2H_5OH) 200 proof, a solvent, batch# 30296HK of >99.5% purity was supplied by Sigma Aldrich. Food grade Stearic acid ($CH_3(CH_2)_{16}COOH$) was ordered from Amazon.

***All equipment and accessories used are included at the end of the appendix.**

Abbreviations:

DIW – deionized water

EtOH – ethanol

HP – hydrogen peroxide

SA – stearic acid

Procedure:

Preparation of 10 M NaOH solution:

1. In a clean glass beaker, weigh out 40g (± 0.02 g) of NaOH.
2. Add DIW upto 100 mL mark to get a 10M solution.
3. Drop in a Teflon stir-bar and allow the solution to go clear.
4. Heat is evolved during the dissolution, hence prepare solution well in advance.
5. Once dissolved, the liquid level usually drops a little. Hence compensate and add DIW to reach the 100 mL mark

Scale up as needed: for eg: 60 g NaOH in 150 mL solution will yield 10M NaOH solution.

Preparation of 20 w/w.% Stearic acid solution:

1. In a clean glass beaker, pour 100 mL of EtOH.
2. Add 20 g of stearic acid.
3. Place on a hot plate at 75^{o}C ± 5^{o}C. Add a Teflon stir-bar and stir on a dual magnetic hotplate/stirrer setup.
4. Once clear i.e. dissolved, drop temperature to 55^{o}C and maintain solution at this temperature to avoid EtOH evaporation.

Preparation of Aluminosilicate slurry (Si:Al = 3:1 by mass)

1. In a clean glass beaker (Pyrex heavy duty thick walled 250 mL), add 30 g SiO_2 (± 0.05 g is OK) and 8.5 g Al_2O_3 (± 0.05 g is OK).
2. Add 17 mL (± 2mL) of NaOH solution (as close as possible). Use spatula for crude mixing of the slurry until all particles are wetted. If necessary, add 3-5 mL of DIW to facilitate mixing. Then mix well with egg whisk aggressively until slurry looks homogenous.
3. Sonicate in the Branson 5800 bath sonicator for 8 mins. Set' duty cycle' to constant. Set the power to low.
4. Once sonication is complete, stir very lightly with egg whisk and then add HP (depending on density desired) and mix well with egg whisk (~ 30s). Add SA (depending on density desired) and mix aggressively with the egg whisk until slurry looks homogenous (~ 2-3min).
5. Pour slurry quickly into the Teflon mold and place it inside the convection oven maintained at 100^{o}C (time of curing is dependent on composition). Do not scrape and pour the slurry stuck to the beaker as they may increase chances of voids in the cured product.

   *use Teflon mold and rings depending on the sample sizes required. Also, pour the slurry partially according to desired height.

   For foams > 0.85 g/cc, slurry column height ~ sample height. However, for foams < 0.5 g/cc, sample height ~ 4X slurry column height. Hence, extra caution is needed in terms of rings/molds used as they need to support the foaming process.

Quantities of chemicals and important parameters for desired densities

Si:Al (by mol)	10 M NaOH (mL)	Power Level	Sonication time (min)	H_2O_2 (g)	Stearic acid (g)	Curing time (hrs)	Density (+ 5%) (g/cm^3)
3:1	17	Low	8	12.48	2.02	12	0.22

Important Precautions:

***Quantites of chemicals

Amounts of SiO_2, Al_2O_3 and NaOH may be a little off as the samples are not that sensitive to these changes. **However, HP and SA solution have to be as accurate as possible for best results**!

***Sonication

Sonication must be done is a heavy duty (thick walled) Pyrex beaker for the appropriate energy to be transferred to the slurry. Thin walled beakers are not very efficient in energy transfer.

In addition, between each sonication cycle, ensure that the sonicator water bath has not warmed up. Hence, it is ideal to change water after every 2 sonication runs.

Post processing of samples:

Samples made of densities < 0.7 g/cc usually develop cracks during the forming process. Thus, for any types of characterization where regular geometries are needed, its essential to cut/sand them as desired.

Sanding is usually done on a 220 grit sandpaper (waterproof) until all edges and surfaces are smooth.

Where sanding was not possible by paper, sanding belt was used (for higher densities). For tough samples that cannot be sanded down, chop saw was used to cut pieces into regular shapes.

Once done, all samples were dried for 12 h in a 100^oC oven.

Store samples in a dry environment as they tend to absorb water.

Sample Key (for thermal analysis)

APPENDIX - B

Equipment/instrumentation/accessories used

Digital weighing scale

Dual hotplate- stirrer (for SA solution)

spatula (crude mixing)

Egg whisk

(thick walled)

(fine, more homogenous mixing)

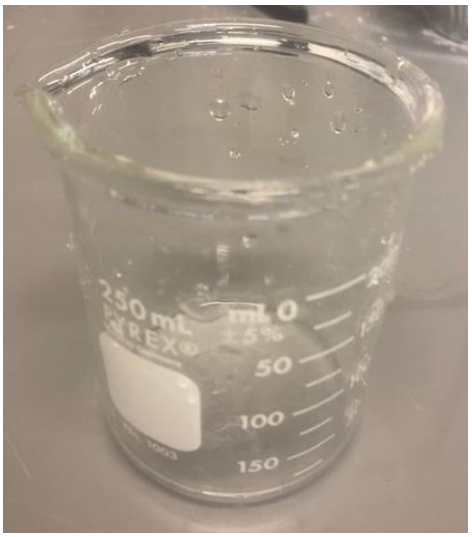

Pyrex beaker

Teflon dishes (3-inch diameter and 0.6-inch-tall) and cylinders (2.1 inch dameter and 0.52-inch-tall) for casting samples

Branson 5800 Bath Sonicator

Convection oven at 100ºC used to cure samples

Branson 5800 Bath Sonicator

(showing ideal settings)

Size to scale comparison of equipment

Sanding belt (to flatten samples)

Chop saw (to cut samples into regular shapes)

REFERENCES

[1] Energy.gov. "Insulation Materials." Accessed June 27, 2021. https://www.energy.gov/energysaver/weatherize/insulation/insulation-materials.

[2] DiPietro, Joseph A. "Chapter 20 - Keys to the Interpretation of Geological History." In *Landscape Evolution in the United States*, edited by Joseph A. DiPietro, 327–44. Boston: Elsevier, 2013. https://doi.org/10.1016/B978-0-12-397799-1.00020-8.

[3] Stapleton, Jill M, Christopher Q Lan, Stephen G Hardcastle, and Glen P Kenny. "THE EFFECT OF WEARING A COOLING VEST TO ALLEVIATE THERMAL STRAIN DURING MODERATE INTENSITY WORK," n.d., 5.

[4] Almeida, Daniel de. "Evaluation of the Thermal Impact from Battery Packs from Electrical Vehicles in Underground Mining Environment," 2019. https://doi.org/10.13140/RG.2.2.14537.39527.

[5] American Geosciences Institute. "How Can Metal Mining Impact the Environment?," November 13, 2014. https://www.americangeosciences.org/critical-issues/faq/how-can-metal-mining-impact-environment.

[6] Kelly Sexsmith. "Characterizing The Long-Term Stability And Porewater Quality Of Uranium Mine... | SRK Consulting." Accessed June 27, 2021. https://www.srk.com/en/publications/characterizing-the-long-term-stability-and-porewater-quality-of-uranium-mine-tailings.

[7] Kossoff, D. "Mine Tailings Dams: Characteristics, Failure, Environmental Impacts, and Remediation." *Applied Geochemistry*, 2014, 17.

[8] Ahmari, Saeed, and Lianyang Zhang. "Production of Eco-Friendly Bricks from Copper Mine Tailings through Geopolymerization." *Construction and Building Materials* 29 (April 1, 2012): 323–31. https://doi.org/10.1016/j.conbuildmat.2011.10.048.

[9] Kiventerä, Jenni. "Alkali Activation as New Option for Gold Mine Tailings Inertization." *Journal of Cleaner Production*, 2018, 9.

[10] Favero, Giancarlo, and Piergiorgio Jobstraibizer. "The Distribution of Aluminum in the Earth: From Cosmogenesis to Sial Evolution." *Coordination Chemistry Reviews* 149 (May 1, 1996): 367–400. https://doi.org/10.1016/S0010-8545(96)90040-5.

[11] Köhler, Th, G. Seifert, and Th Frauenheim. "Silicon-Based Nanotubes: A Theoretical Investigation." In *Silicon Chemistry*, 226–41. John Wiley & Sons, Ltd, 2003. https://doi.org/10.1002/9783527610761.ch17.

[12] Sherman, John D. "Synthetic Zeolites and Other Microporous Oxide Molecular Sieves." *Proceedings of the National Academy of Sciences* 96, no. 7 (March 30, 1999): 3471–78.

[13] Rao, P. R., K. Muralidharan, M. Momayez, Keith A. Runge, and D. A. Loy. "Direct Foaming Driven Synthesis and Thermophysical Characterization of Silica-Alumina Foams: Applications for Thermal Insulation." *Ceramics International* 46, no. 8, Part A (June 1, 2020): 10431–41. https://doi.org/10.1016/j.ceramint.2020.01.042.

[14] Zhang, Jingchao, Fei Xu, Yang Hong, Qingang Xiong, and Jianming Pan. "A Comprehensive Review on the Molecular Dynamics Simulation of the Novel Thermal Properties of Graphene." *RSC Advances* 5, no. 109 (October 20, 2015): 89415–26. https://doi.org/10.1039/C5RA18579C.

[15] Gupta, Gaurav. "NUMERICAL METHODS TO ESTIMATE THERMAL CONDUCTIVITY OF POROUS ALUMINOSILICATES," n.d., 38.

[16] Guajardo-Cuéllar, Alejandro, David B. Go, and Mihir Sen. "Evaluation of Heat Current Formulations for Equilibrium Molecular Dynamics Calculations of Thermal Conductivity." *The Journal of Chemical Physics* 132, no. 10 (March 14, 2010): 104111. https://doi.org/10.1063/1.3358338.

[17] Chen, Jie, Gang Zhang, and Baowen Li. "How to Improve The Accuracy of Equilibrium Molecular Dynamics For Computation of Thermal Conductivity?" *Physics Letters, Section A: General, Atomic and Solid State Physics* 374 (May 25, 2010). https://doi.org/10.1016/j.physleta.2010.03.067.

[18] Müller-Plathe, Florian. "A Simple Nonequilibrium Molecular Dynamics Method for Calculating the Thermal Conductivity." *The Journal of Chemical Physics* 106, no. 14 (August 31, 1998): 6082. https://doi.org/10.1063/1.473271.

[19] Sadat, Mohammad Rafat, Stefan Bringuier, Krishna Muralidharan, Keith Runge, Abu Asaduzzaman, and Lianyang Zhang. "An Atomistic Characterization of the Interplay between Composition, Structure and Mechanical Properties of Amorphous Geopolymer Binders." *Journal of Non-Crystalline Solids* 434 (February 15, 2016): 53–61. https://doi.org/10.1016/j.jnoncrysol.2015.11.022.

[20] Hao, Qing. "Beautiful Vibrations - Understand Phonons for Heat Transfer." *Journal of Aeronautics & Aerospace Engineering* 01, no. 01 (2012). https://doi.org/10.4172/2168-9792.1000e102.

[21] "Conduction Heat Transfer - an Overview | ScienceDirect Topics." Accessed July 16, 2021. https://www.sciencedirect.com/topics/engineering/conduction-heat-transfer.

[22] Wang, Zizhen, Ruihe Wang, Tianyang Li, Hao Qiu, and Feifei Wang. "Pore-Scale Modeling of Pore Structure Effects on P-Wave Scattering Attenuation in Dry Rocks." *PLOS ONE* 10, no. 5 (May 11, 2015): e0126941. https://doi.org/10.1371/journal.pone.0126941.